5 Leptonic Processes

One important topic of GRB physics is describing how the photons of different energies are emitted. This is related to various radiation (more generally interaction) mechanisms of leptons (electrons, positrons, muons, etc.) and hadrons (protons, neutrons, pions, etc.). This chapter gives a detailed treatment of the leptonic processes that are most relevant to GRBs. Hadronic processes will be discussed in the next chapter (Chapter 6).

Leptonic interactions can be understood in two different ways. From the classical point of view, a charged particle radiates electromagnetic waves when it is *accelerated* (Rybicki and Lightman, 1979). A charged particle can be accelerated by either an electric field or a magnetic field, so in general one has three main radiation mechanisms: *bremsstrahlung* (acceleration in a Coulomb E field), *synchrotron* (acceleration in a B field), and *inverse Compton* (acceleration in an alternating E and B field, or an electromagnetic wave field). When quantum mechanics is taken into account, photons are also produced when electrons jump from a higher energy level to a lower one.

From the quantum electrodynamics (QED) point of view, photons are the boson mediator of electromagnetic (EM) interactions. All the radiation processes can be understood as EM interactions that exchange photons. Within this picture, not only can photons be generated by leptons, they can also interact with each other, or with electric or magnetic fields, making leptons. The condition is that both energy and momentum of the system must be conserved.

Due to the relativistic nature of GRBs, in the sites of GRB prompt emission and afterglow, the internal energy (effective temperature) is usually too high for the survival of any molecules or atoms, so that atomic, molecular line emission and absorption are usually not relevant.[1] In the following, several non-thermal radiation mechanisms are discussed in turn. Synchrotron radiation (§5.1) and inverse Compton scattering (§5.2) are treated in great detail, whereas bremsstrahlung (§5.3) and pair production and annihilation (§5.4) are discussed more briefly.

5.1 Synchrotron Radiation

Synchrotron radiation, electromagnetic radiation of relativistic particles in a magnetic field, is widely believed to power GRB afterglow, and to be the leading candidate radiation

[1] There were reports on the possible detections of metal lines in the X-ray afterglow data of some GRBs in the pre-*Swift* era (e.g. Piro et al., 2000; Reeves et al., 2002), which stimulated theoretical investigations on how to produce emission line features in GRBs (e.g. Rees and Mészáros, 2000; Vietri et al., 2001). However, in the *Swift* era, no line feature was observed by the XRT, which is supposed to detect those pre-*Swift* features should they be real.

mechanism of GRB prompt emission as well. In the following, we will progressively introduce various physical ingredients that shape the observed synchrotron spectrum.

5.1.1 Emission from a Single Particle in a Uniform B Field

A particle with charge q, mass m, and Lorentz factor γ gyrating in a magnetic field B with an incident angle α with respect to the field line emits a *synchrotron spectrum* in the form of (Rybicki and Lightman, 1979)

$$P(\omega,\gamma)=\frac{\sqrt{3}q^3B\sin\alpha}{2\pi mc^2}F\left(\frac{\omega}{\omega_{\rm ch}}\right), \tag{5.1}$$

or

$$P(\nu,\gamma)=\frac{\sqrt{3}q^3B\sin\alpha}{mc^2}F\left(\frac{\nu}{\nu_{\rm ch}}\right), \tag{5.2}$$

where $P(\omega,\gamma)=dE/(dtd\omega)$ is the emitted power per unit angular frequency ($d\omega$), $P(\nu,\gamma)=dE/(dtd\nu)$ is the emitted power per unit frequency ($d\nu$),

$$\omega_{\rm ch}=\frac{3\gamma^2qB\sin\alpha}{2mc}=\frac{3}{2}\gamma^2\frac{qB_\perp}{mc} \tag{5.3}$$

is the *characteristic angular frequency* (which depends on γ and the perpendicular magnetic field strength $B_\perp=B\sin\alpha$),

$$\nu_{\rm ch}=\frac{\omega_{\rm ch}}{2\pi}=\frac{3}{4\pi}\gamma^2\frac{qB_\perp}{mc} \tag{5.4}$$

is the corresponding characteristic emission frequency, and c is the speed of light. The function

$$F(x)\equiv x\int_x^\infty K_{5/3}(\xi)d\xi \tag{5.5}$$

reaches its maximum at $F_{\rm max}(0.29)\simeq 0.92$, and has the asymptotic behavior

$$F(x)\sim\begin{cases}\frac{4\pi}{\sqrt{3}\Gamma(1/3)}\left(\frac{x}{2}\right)^{1/3}\sim 2.15x^{1/3}, & x\ll 1,\\ \left(\frac{\pi}{2}\right)^{1/2}x^{1/2}e^{-x}\sim 1.25x^{1/2}e^{-x}, & x\gg 1,\end{cases} \tag{5.6}$$

where $\Gamma(1/3)$ is the gamma function of argument $1/3$. So the synchrotron spectrum for individual particles, $P(\nu,\gamma)$, has a $\propto\nu^{1/3}$ segment at low energies and an exponential cutoff at high energies (the $\nu^{1/2}$ increase is essentially suppressed by the exponential factor $\exp(-\nu/\nu_{\rm ch})$). See top left panel of Fig. 5.1.

Integrating over ν, the total *emission power* of the particle reads

$$P(\gamma)=2\sigma_{\rm T}c\gamma^2\beta_\perp^2U_B, \tag{5.7}$$

where $\beta_\perp=v\sin\alpha/c$ is the dimensionless perpendicular velocity of the particle, $U_B=B^2/8\pi$ is the magnetic field energy density in the emission region, and

$$\sigma_{\rm T}=\frac{8\pi}{3}\left(\frac{q^2}{mc^2}\right)^2. \tag{5.8}$$

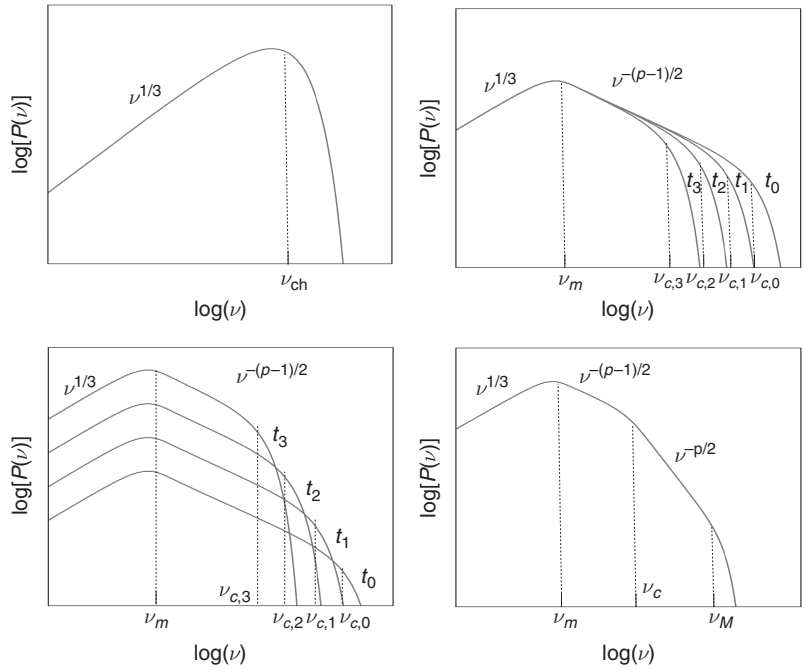

Figure 5.1 Synchrotron spectra of electrons. *Top left:* Spectrum for one single electron (or mono-energetic electrons) in a uniform magnetic field. *Top right:* Spectrum of an ensemble of electrons with a power-law energy distribution with an impulsive injection. A power-law segment is formed, with the high-energy end decreasing with time due to synchrotron cooling. *Lower left:* When continuous injection of fresh particles is considered, the observed spectrum is a superposition of many spectra produced by electrons with different "ages", forming a new segment. Notice that, for illustration purposes, the injection rate of electrons is adopted to decrease with time. However, the conclusion applies to more general cases (e.g. the injection rate of electrons remains the same or increases with time). *Lower right:* Putting all these effects together, the spectrum can be described by a three-segment broken power law. Figure courtesy Wei Deng.

For electrons, one has $q = e$ and $m = m_e$, so that

$$\sigma_{\rm T} = \sigma_{{\rm T},e} \equiv \frac{8\pi}{3}\left(\frac{e^2}{m_e c^2}\right)^2 \simeq 6.65 \times 10^{-25}\ {\rm cm}^2. \tag{5.9}$$

This is the electron *Thomson cross section*. For protons, one has

$$\sigma_{{\rm T},p} = \sigma_{{\rm T},e}\left(\frac{m_e}{m_p}\right)^2 \simeq 1.97 \times 10^{-31}\ {\rm cm}^2. \tag{5.10}$$

Since the emitting leptons are essentially electrons and positrons, in the rest of the book we adopt $q = e$ and $m = m_e$ unless otherwise stated, and define $\sigma_{\rm T}$ as the electron Thomson cross section (Eq. (5.9)).

5.1.2 Emission from a Population of Particles with a Power-Law Energy Distribution in a Uniform B Field

From an astrophysical source, rather than emission from a single particle, what we observe is the collected emission of a population of particles emitting in a magnetic field whose configuration is unknown. The observed spectrum therefore depends on the particle energy distribution and the magnetic field configuration.

The particle energy distribution is usually assumed to be a power law. The case for shock acceleration has been discussed in §4.4. Magnetic reconnections also tend to accelerate particles to a power-law distribution, maybe with a harder spectral index (e.g. Sironi and Spitkovsky, 2014; Guo et al., 2014). In the following, we introduce a power-law distribution of the particle energy with an energy spectral index p, i.e.

$$N(E)dE = C_E E^{-p} dE\,, \quad E_m < E < E_M, \tag{5.11}$$

or, in terms of the Lorentz factor of relativistic particles,

$$N(\gamma)d\gamma = C_\gamma \gamma^{-p} d\gamma, \quad \gamma_m < \gamma < \gamma_M, \tag{5.12}$$

where $C_\gamma = C_E (m_e c^2)^{(1-p)}$, and γ_M and γ_m are the maximum and minimum Lorentz factors of the electron energy distribution, respectively.

The observed spectrum of an ensemble of particles with a power-law distribution is the integral of the synchrotron spectra of individual particles over the energy distribution of the particles. We consider the simplest case, i.e. a uniform B field with a constant impact angle α for all the electrons (constant $B_\perp$). One has (Rybicki and Lightman 1979, see Exercise 5.1)

$$\begin{aligned} F_\nu &\propto \int_{\gamma_m}^{\gamma_M} P(\nu,\gamma) C_\gamma \gamma^{-p} d\gamma \\ &\simeq \frac{\sqrt{3} e^3 B_\perp C_\gamma}{2 m_e c^2} \left(\frac{3eB_\perp}{4\pi m_e c}\right)^{\frac{p-1}{2}} \nu^{-\frac{p-1}{2}} \int_0^\infty F(x) x^{(p-3)/2} dx \\ &= \frac{\sqrt{3} e^3 B_\perp C_\gamma}{m_e c^2 (p+1)} \left(\frac{3eB_\perp}{2\pi m_e c}\right)^{\frac{p-1}{2}} \Gamma\left(\frac{p}{4}+\frac{19}{12}\right) \Gamma\left(\frac{p}{4}-\frac{1}{12}\right) \nu^{-\frac{p-1}{2}} \\ &\propto \nu^{-\frac{p-1}{2}}. \end{aligned} \tag{5.13}$$

Here

$$x \equiv \frac{\omega}{\omega_{\rm ch}} = \frac{\nu}{\nu_{\rm ch}} = \frac{2}{3} \frac{m_e c \omega}{e B_\perp \gamma^2} = \frac{4\pi}{3} \frac{m_e c \nu}{e B_\perp \gamma^2}. \tag{5.14}$$

For a fixed frequency ν, the minimum and maximum values of x are $x_m = (4\pi/3) \times (m_e c\nu / e B_\perp \gamma_M^2) \ll 1 \sim 0$, and $x_M = (4\pi/3)(m_e c\nu / e B_\perp \gamma_m^2) \gg 1 \sim \infty$. The integral

$$\int_0^\infty x^\mu F(x) dx = \frac{2^{\mu+1}}{(\mu+2)} \Gamma\left(\frac{\mu}{2}+\frac{7}{3}\right) \Gamma\left(\frac{\mu}{2}+\frac{2}{3}\right) \tag{5.15}$$

has been applied to derive Eq. (5.13), where $\Gamma(y)$ is the gamma function of argument y.

As a result, for a population of electrons with a power-law distribution defined by their minimum and maximum Lorentz factors γ_m and γ_M, the synchrotron radiation spectrum has three segments (top right panel of Fig. 5.1):

$$F_\nu \propto \begin{cases} \nu^{1/3}, & \nu < \nu_m = \frac{3}{4\pi}\gamma_m^2 \frac{eB_\perp}{m_e c}, \\ \nu^{-(p-1)/2}, & \nu_m < \nu < \nu_M = \frac{3}{4\pi}\gamma_M^2 \frac{eB_\perp}{m_e c}, \\ \nu^{1/2} e^{-(\nu/\nu_M)}, & \nu > \nu_M. \end{cases} \tag{5.16}$$

5.1.3 Emission from a Population of Particles with a Power-Law Energy Distribution in a Random B Field

In many astrophysical environments, the magnetic fields in the emission region are randomized. For example, the magnetic fields generated in relativistic shocks through plasma instabilities (§4.5) have random orientations. This also applies to the outflow regions of magnetic reconnection events.

Synchrotron Radiation in a Random B Field

In a random magnetic field, the synchrotron emission power of a single particle becomes

$$P(\gamma) = \frac{4}{3}\sigma_{\rm T} c \gamma^2 \beta^2 U_B, \tag{5.17}$$

where the pitch angle in Eq. (5.7) has been averaged out by $\langle \beta_\perp^2 \rangle = 2\beta^2/3$.

The emission spectrum of an individual particle depends on how its trajectory differs from that of synchrotron emission in a uniform field. A relevant criterion is whether the particle gyrates enough to make its relativistic beam (with an angle $1/\gamma$) sweep an angle much larger than $1/\gamma$. The relevant parameter (Medvedev, 2000) is the ratio between the "particle deflection angle" (i.e. the ratio between the typical correlation scale of the random magnetic fields λ_B [$\lambda_B = \infty$ for a uniform field] and the Larmor [gyration] radius $r_B = \gamma m_e c^2/eB_\perp$) and the emission beam angle $1/\gamma$, i.e.

$$\delta = \gamma \frac{\lambda_B}{r_B}\,. \tag{5.18}$$

If $\delta \gg 1$, the particles make large gyrations so that the emission spectrum is very close to the synchrotron form (Eq. (5.1)), with $B_\perp$ replaced by the average field strength B. The spectrum of an ensemble of particles with a power-law distribution is therefore

$$F_\nu \propto \begin{cases} \nu^{1/3}, & \nu < \nu_m = \frac{3}{4\pi}\gamma_m^2 \frac{eB}{m_e c}, \\ \nu^{-(p-1)/2}, & \nu_m < \nu < \nu_M = \frac{3}{4\pi}\gamma_M^2 \frac{eB}{m_e c}, \\ \nu^{1/2} e^{-(\nu/\nu_M)}, & \nu > \nu_M, \end{cases} \tag{5.19}$$

which is Eq. (5.16) with $B_\perp$ replaced by B.

Jitter Radiation

On the other hand, if $\delta \ll 1$, the magnetic field correlation scale is too small so that the particles barely gyrate and essentially "jitter" in the random fields. A comparison between synchrotron and jitter radiation is illustrated in Fig. 5.2.

The emission spectrum of such *jitter radiation* is somewhat different from that of synchrotron radiation. Instead of Eq. (5.3), the *characteristic angular frequency* of jitter emission is (Medvedev, 2000)

$$\omega_j = \gamma^2 \frac{c}{\lambda_B} = \frac{2}{3}\frac{\omega_{\rm ch}}{\delta} \gg \omega_{\rm ch}. \tag{5.20}$$

The spectral slope for $\omega < \omega_j$ depends on the angle between the observer's viewing direction and the direction of the bulk motion (Medvedev, 2006). If the viewing angle is "head-on" (i.e. the angle is 0 in both comoving and lab frames), the spectral index is 1. If the viewing angle is "edge-on" in the comoving frame (i.e. the angle is $\pi/2$ in the comoving frame and $\sim 1/\Gamma$ in the lab frame, where Γ is the bulk Lorentz factor of the emission region), the spectral index is 0. For intermediate viewing angles, the spectral slope is initially 1 right before ω_j but breaks to 0 far below ω_j. The spectral shape above the peak ω_j is a steep power law with the index ζ depending on the unknown turbulence spectrum of the magnetic fields.

Integrating over the spectrum, the *emission power* of a single particle of jitter emission has the identical form as that of synchrotron emission (Eq. (5.17)) (Medvedev, 2000).

For a power-law distribution of particle energies, the emission spectrum is also a power law with $F_\nu \propto \nu^{-(p-1)/2}$ based on the similar argument to the synchrotron emission treatment. The overall spectrum reads

$$F_\nu \propto \begin{cases} \nu^{\alpha}, & \nu < \nu_{j,m} = (2\pi)^{-1}\gamma_m^2(c/\lambda_B), \\ \nu^{-(p-1)/2}, & \nu_{j,m} < \nu < \nu_{j,M} = (2\pi)^{-1}\gamma_M^2(c/\lambda_B), \\ \nu^{1/2}e^{-(\nu/\nu_{j,M})}, & \nu > \nu_{j,M}, \end{cases} \tag{5.21}$$

with $\alpha = 0$ for "edge-on", and $\alpha = 1$ for "head-on".

Particle-in-cell (PIC) simulations (Sironi and Spitkovsky, 2009b) suggest that the random magnetic field configuration in collisionless shocks is fully consistent with being in

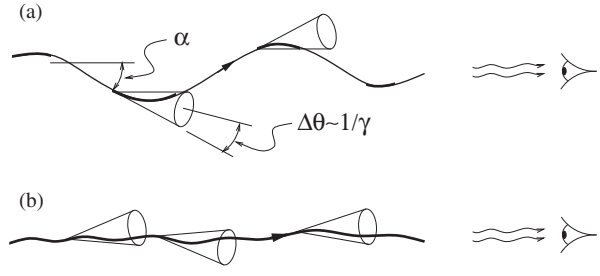

Figure 5.2 A comparison between synchrotron (a) and jitter (b) radiation. Reproduced from Figure 1 in Medvedev (2000) with permission. ©AAS.

the *synchrotron regime*, *not* in the *jitter regime*. It remains interesting to investigate whether jitter radiation is relevant in the outflow regions of magnetic reconnection events.

5.1.4 Cooling

A relativistic particle loses energy (or *cools*) via various radiation mechanisms. The characteristic *cooling time scale* can be estimated by its energy divided by its emission power. The *synchrotron cooling time* of a relativistic particle with energy γmc^2 in a magnetic field with energy density $U_B = B^2/8\pi$ can be written as

$$\tau(\gamma) = \frac{\gamma m_e c^2}{\frac{4}{3}\gamma^2 \sigma_{\rm T} c \beta^2 U_B} = \frac{6\pi m_e c}{\gamma \sigma_{\rm T} \beta^2 B^2}. \tag{5.22}$$

One can see that more energetic particles have shorter cooling time scales ($\tau(\gamma) \propto \gamma^{-1}$). At an epoch t after the acceleration of an ensemble of particles with a power-law distribution, the *cooling energy* or *cooling Lorentz factor* of the particles above which particles have lost most of their energies is defined by $t = \tau(\gamma_c)$, so that

$$\gamma_c(t) \simeq \frac{6\pi m_e c}{\sigma_{\rm T} B^2 t}, \tag{5.23}$$

where $\beta \sim 1$ has been adopted. For an impulsively accelerated particle population, at any epoch t, the cooling energy defines the maximum energy of the population, so that $\gamma_M \simeq \gamma_c$ (upper right panel of Fig. 5.1).

5.1.5 Continuous Acceleration

In many astrophysical systems, fresh particles are continuously accelerated. For example, during the propagation of a relativistic shock new energetic particles are constantly accelerated at the shock front. In order to calculate the time-dependent synchrotron emission spectrum from the system, the electron energy distribution as a function of time has to be solved self-consistently by properly considering injection of new particles, cooling and heating of old particles, as well as diffusive loss of particles from the source. In general, continuously injecting fresh electrons into a system would make electrons with different "ages" emit simultaneously, giving rise to a new power-law segment defined by the cooling frequency ν_c (lower left panel of Fig. 5.1).

Continuity Equation in Energy Space

Neglecting the spatial distributions of particles, the distribution and time evolution of particles in energy space for an open system of particles is the Fokker–Planck equation (Chandrasekhar, 1943), which, under reasonable approximations, takes the form (e.g. Park and Petrosian, 1995)

$$\frac{\partial N(\gamma,t)}{\partial t} = \frac{\partial}{\partial \gamma}\left[D(\gamma)\frac{\partial N(\gamma,t)}{\partial \gamma}\right] - \frac{\partial}{\partial \gamma}[\dot{\gamma}(\gamma) N(\gamma,t)] - \frac{N(\gamma,t)}{T(\gamma)} + Q(\gamma,t). \tag{5.24}$$

Here, $N(\gamma, t)$ is the particle number within the energy interval $(\gamma, \gamma + d\gamma)$ at time t, $D(\gamma)$ is the diffusion coefficient in energy space, $\dot{\gamma}(\gamma)$ is the energy gain (for energy loss, $\dot{\gamma}(\gamma) < 0$) rate of the particles with energy γ, $T(\gamma)$ is the typical escape time scale of the particles with energy γ, and $Q(\gamma, t)$ is the source term, denoting the energy-dependent injection rate of fresh particles into the system.

In the GRB problem the diffusion term is negligible, and usually $T(\gamma) \gg t$ so that the continuity equation in energy space is simplified as

$$\frac{\partial N(\gamma, t)}{\partial t} = -\frac{\partial}{\partial \gamma}[\dot{\gamma}(\gamma) N(\gamma, t)] + Q(\gamma, t) \,. \tag{5.25}$$

Approximate Scalings

Let us assume that the injection term carries the power-law form:

$$Q(\gamma, t) = Q_0(t) \left[\frac{\gamma}{\gamma_m(t)}\right]^{-p}, \quad \gamma_m(t) < \gamma < \gamma_M(t), \tag{5.26}$$

as is expected for shock or reconnection systems. At any epoch t, it is informative to compare the minimum injection Lorentz factor γ_m and the cooling Lorentz factor γ_c. If $\gamma_c > \gamma_m$, only a small fraction of particles have cooled. This is the *slow cooling* regime. On the other hand, if $\gamma_c < \gamma_m$ is satisfied, all the injected particles are immediately cooled. This is the *fast cooling* regime.

Even though $N(\gamma, t)$ should be solved numerically, one can estimate the power-law index of electrons in different energy regimes. It is informative to make some order-of-magnitude estimates: the left hand side of Eq. (5.25) is of the order $\sim N/t$. Assuming cooling only (no extra heating once particles are accelerated), one has $\dot{\gamma} \sim -\gamma/\tau(\gamma)$ so that the first term on the right hand side of Eq. (5.25) is of the order $\sim N/\tau$. One may then discuss four cases:

1. $\gamma_m < \gamma < \gamma_c < \gamma_M$: This is the slow cooling regime ($\gamma_m < \gamma_c$) below the cooling energy γ_c. One has $\tau(\gamma) \gg t$ so that one can neglect the first term on the right hand side of Eq. (5.25). Therefore $N(\gamma, t) \simeq \int Q(\gamma, t) dt \propto \gamma^{-p}$.
2. $\gamma_m < \gamma_c < \gamma < \gamma_M$: This is the slow cooling regime above γ_c. One therefore has $\tau(\gamma) \ll t$, and should instead neglect the left hand side of Eq. (5.25). Recalling that $\dot{\gamma} \propto -\gamma^2$ (Eq. (5.17)), one can derive $N(\gamma, t) \simeq \int Q(\gamma, t) d\gamma \cdot \gamma^{-2} \propto \gamma^{-p+1}\gamma^{-2} \propto \gamma^{-(p+1)}$. This dependence can be also derived using the approximate relation $N/\tau \sim Q$, so that $N \sim Q\tau \propto \gamma^{-(p+1)}$.
3. $\gamma_c < \gamma < \gamma_m < \gamma_M$: This is the fast cooling case, so that all the electrons cool within the dynamical time scale. Since $\gamma_c < \gamma$, again one has $\tau(\gamma) \ll t$, so that the left hand side of Eq. (5.25) is neglected. Since $\gamma < \gamma_m$, one has $Q = 0$. Therefore $\dot{\gamma} N(\gamma, t) \propto$ constant, or $N(\gamma, t) \propto \gamma^{-2}$.
4. $\gamma_c < \gamma_m < \gamma < \gamma_M$: This case is similar to case (2), so that $N(\gamma, t) \propto \gamma^{-(p+1)}$.

In summary, a system with continuous cooling and fresh particle injection has the following particle energy distribution at any epoch t:

$$N(\gamma, t) \propto \begin{cases} \gamma^{-p}, & \gamma_m < \gamma < \gamma_c < \gamma_M, \\ \gamma^{-(p+1)}, & \gamma_m < \gamma_c < \gamma < \gamma_M, \end{cases} \tag{5.27}$$

for slow cooling ($\gamma_m < \gamma_c$), and

$$N(\gamma, t) \propto \begin{cases} \gamma^{-2}, & \gamma_c < \gamma < \gamma_m < \gamma_M, \\ \gamma^{-(p+1)}, & \gamma_c < \gamma_m < \gamma < \gamma_M, \end{cases} \tag{5.28}$$

for fast cooling ($\gamma_c < \gamma_m$), where γ_m, γ_c, and γ_M are instantaneous values of the minimum injection, cooling, and maximum injection energies of electrons at the epoch t. This applies to any cooling mechanism that has $\dot{\gamma} \propto \gamma^2$, which is the case for synchrotron radiation and also for inverse Compton scattering, as discussed below in §5.2. Since the emitted spectrum takes the form $F_\nu \propto \nu^{-(p-1)/2}$, the emission spectrum of the system is

$$F_\nu \propto \begin{cases} \nu^{-(p-1)/2}, & \nu_m < \nu < \nu_c < \nu_M, \\ \nu^{-p/2}, & \nu_m < \nu_c < \nu < \nu_M, \end{cases} \tag{5.29}$$

for slow cooling, and

$$F_\nu \propto \begin{cases} \nu^{-1/2}, & \nu_c < \nu < \nu_m < \nu_M, \\ \nu^{-p/2}, & \nu_c < \nu_m < \nu < \nu_M, \end{cases} \tag{5.30}$$

for fast cooling, where ν_m, ν_c, and ν_M are the corresponding characteristic synchrotron emission frequencies for the electrons with Lorentz factors γ_m, γ_c, and γ_M, respectively.

Fast Cooling in a Decaying Magnetic Field

In the above approximate derivation of a fast cooling spectrum, a constant magnetic field B in the emission region has been assumed so that the cooling rate $\dot{\gamma}$ depends only on γ. In GRB problems, usually a conical jet is assumed. As the jet streams outwards, due to magnetic flux conservation the magnetic field strength in the emission region continuously decreases (see details in Chapter 7). In the fast cooling regime ($\gamma_c < \gamma_m$), the electron spectrum no longer carries the simple $\propto \gamma^{-2}$ form, but is curved because electrons injected at different epochs underwent different cooling histories in different magnetic fields (Uhm and Zhang, 2014b).

Figure 5.3 shows the deviation of electron and photon spectral indices from the nominal values ($N(\gamma) \propto \gamma^{-2}$ and $F_\nu \propto \nu^{-1/2}$) for fast cooling electrons with different profiles of magnetic field decay as a function of radius, e.g.

$$B(r) = B_0 \left(\frac{r}{r_0}\right)^{-b}, \tag{5.31}$$

with $b = 0, 1, 1.2, 1.5$, respectively. One can see that, for the three b values under consideration, the electron spectra are time dependent and get harder at later epochs. The reason is that the electrons injected earlier underwent stronger synchrotron cooling in a stronger magnetic field than the electrons injected later. The farther down the injection energy γ_m, the older the electron population, hence the more stretched the electron energy bin (due to more significant cooling). For certain parameters, $N(\gamma) \sim \gamma^{-1}$ below γ_m can be reached, which is the right spectral shape to explain the typical Band-function spectrum of GRB prompt emission with the standard low-energy spectral index $\alpha \sim -1$ (Uhm and Zhang, 2014b).

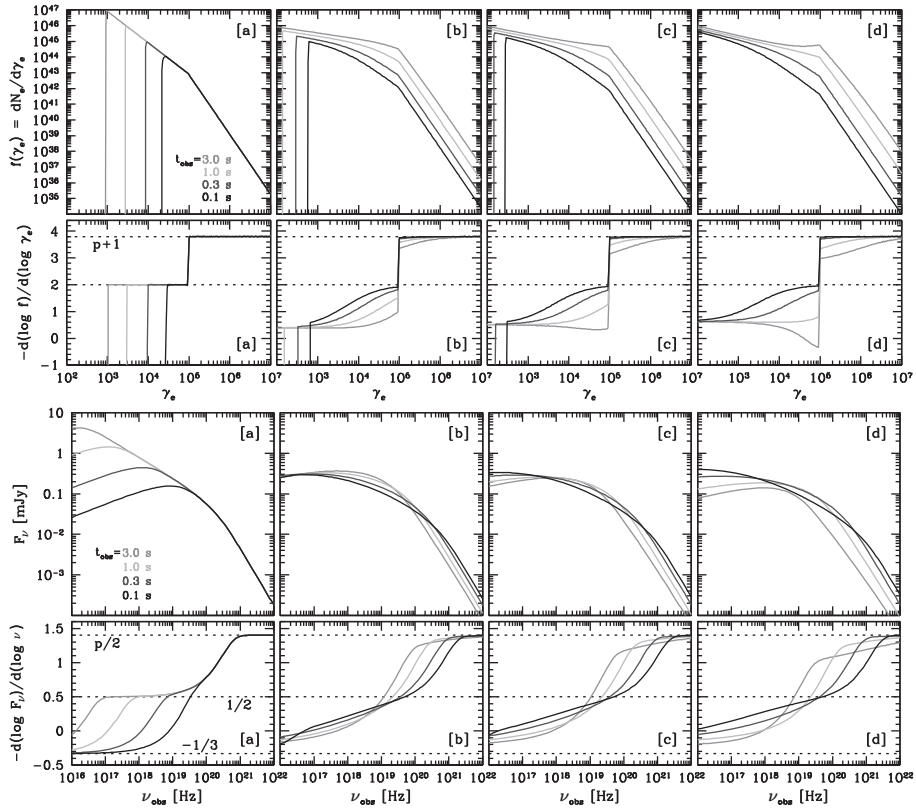

Figure 5.3 Fast cooling electron spectra (*upper panel*) and synchrotron photon spectra (*lower panel*) in a decaying magnetic field. Models [a], [b], [c], [d] have $b = 0, 1, 1.2, 1.5$, respectively. Other model parameters: $\gamma_m = 10^5$, Lorentz factor $\Gamma = 300$, comoving-frame magnetic field strength $B'_0 = 30$ G, $r_0 = 10^{15}$ cm, $p = 2.8$, and the injection rate $R_{\rm inj} = \int_{\gamma_m}^{\infty} Q(\gamma_e, t')d\gamma_e = 10^{47}\ {\rm s}^{-1}$. From Uhm and Zhang (2014b). A black and white version of this figure will appear in some formats. For the color version, please refer to the plate section.

An asymptotic electron spectral index can be derived for fast cooling in a decaying B field for $b > 1/2$ (Uhm and Zhang, 2014b). Let us consider the cooling equation of an electron with Lorentz factor γ_e, i.e.

$$\frac{d\gamma_e m_e c^2}{dt} \simeq -\frac{4}{3}\gamma_e^2 \sigma_{\rm T} c \frac{B^2}{8\pi}. \tag{5.32}$$

Dividing by γ_e^2 from both sides, one can solve the evolution of $1/\gamma_e$, i.e.

$$\frac{d}{dt}\left(\frac{1}{\gamma_e}\right) \simeq \frac{\sigma_{\rm T}}{6\pi m_e c} B^2 = a t^{-2b}, \tag{5.33}$$

where a is a constant, and Eq. (5.31) has been used with $r \propto t$ introduced (which is valid for a constant Lorentz factor). For an electron injected at an initial time t_i with initial Lorentz factor $\gamma_{e,i}$, at a later epoch t_j, its Lorentz factor $\gamma_{e,j}$ is solved as

$$\gamma_{e,j} = \left[\frac{1}{\gamma_{e,i}} + \frac{a}{1-2b}\left(t_j^{1-2b} - t_i^{1-2b}\right)\right]^{-1}. \tag{5.34}$$

When $t_j \gg t_i$, one has $\gamma_{e,j} \ll \gamma_{e,i}$. For $b > 1/2$, one can drop out the $1/\gamma_{e,i}$ term and the t_j^{1-2b} term in Eq. (5.34). Differentiating the equation, one gets $d\gamma_{e,j} = \frac{2b-1}{a} t_i^{2b-2} dt_i$. Considering continuous injection of electrons with a rate $R_{\rm inj} = dN/dt_i$, one can replace dt_i by dN, and eventually derive the asymptotic electron energy spectrum

$$\frac{dN}{d\gamma_{e,j}} = R_{\rm inj}\left(\frac{a}{2b-1}\right)^{\frac{1}{2b-1}} \gamma_{e,j}^{-\frac{2b-2}{2b-1}}. \tag{5.35}$$

For a constant $R_{\rm inj}$, the asymptotic spectral index is $\tilde{p}_{\rm a} = \frac{2b-2}{2b-1}$, which significantly deviates from the standard -2 value for a constant B. Considering adiabatic cooling and a varying $R_{\rm inj}$ can further affect the asymptotic spectral index, so that a variety of photon indices can be reproduced (Uhm and Zhang, 2014b; Geng et al., 2018).

5.1.6 Self-Absorption

Source Function

In general, the solution to a radiation transfer equation takes the form (Rybicki and Lightman, 1979)

$$\begin{aligned} I_\nu &= I_\nu(0)e^{-\tau_\nu} + S_\nu(1-e^{-\tau_\nu}) \\ &\simeq \begin{cases} I_\nu(0), & \tau_\nu \ll 1, \\ S_\nu, & \tau_\nu \gg 1. \end{cases} \end{aligned} \tag{5.36}$$

Here $I_\nu(0)$ is the original specific intensity, which is also the observed one if $\tau_\nu \ll 1$; while $S_\nu = j_\nu/\alpha_\nu$ is the source function, which becomes important in defining the observed I_ν when $\tau_\nu \gg 1$ is satisfied.

The generic absorption coefficient for any radiation mechanism at the emission frequency $\nu = \omega/2\pi$ is (Rybicki and Lightman, 1979)

$$\alpha_\nu = -\frac{1}{8\pi\nu^2 m_e}\int_{\gamma_m}^{\gamma_{\rm M}} d\gamma P(\gamma,\nu)\gamma^2 \frac{\partial}{\partial\gamma}\left[\frac{N(\gamma)}{\gamma^2}\right], \tag{5.37}$$

where $P(\gamma,\nu)$ is the specific radiation power of electrons with Lorentz factor γ at frequency ν. This expression was derived using the Einstein A, B coefficients and relations, with an assumption $h\nu \ll \gamma mc^2$. We refer to §6.8 of Rybicki and Lightman (1979) for details.

For a power-law distribution of electrons (Eq. (5.12)) and for standard synchrotron radiation (Eq. (5.1)), the absorption coefficient can be written as

$$\alpha_\nu = \frac{p+2}{8\pi m_e} C_\gamma \nu^{-2} \int_{\gamma_m}^{\gamma_M} \frac{\sqrt{3}e^3 B_\perp}{m_e c^2} F(x)\gamma^{-(p+1)} d\gamma. \tag{5.38}$$

The outcome of the integration depends on whether the electrons whose characteristic synchrotron frequency is ν have a Lorentz factor $\gamma(\nu)$ in the regime of (γ_m, γ_M). Notice that here the minimum Lorentz factor γ_m of electrons has a more general meaning. It could

be the injection minimum energy γ_m for slow cooling, or the cooling energy γ_c for fast cooling.

If $\gamma_m \ll \gamma(\nu) \ll \gamma_M$, one can integrate Eq. (5.38) for the variable x (defined in Eq. (5.14)) over the range $x_m = x(\gamma_M) \ll 1$ and $x_M = x(\gamma_m) \gg 1$. Using Eq. (5.15), one can derive (Exercise 5.2)

$$\begin{aligned}\alpha_\nu &= \frac{\sqrt{3}e^3}{8\pi m_e^2 c^2}\left(\frac{3e}{2\pi m_e c}\right)^{p/2} C_\gamma B_\perp^{(p+2)/2}\Gamma\left(\frac{3p+2}{12}\right)\Gamma\left(\frac{3p+22}{12}\right)\nu^{-(p+4)/2} \\ &\simeq \left[1.0\times 10^4\cdot(8.4\times 10^6)^{p/2}\right]\ \mathrm{cm}^{-1} \\ &\quad\times C_\gamma B_\perp^{(p+2)/2}\Gamma\left(\frac{3p+2}{12}\right)\Gamma\left(\frac{3p+22}{12}\right)\nu^{-(p+4)/2}. \end{aligned} \tag{5.39}$$

Here the numerical factor is for electrons in c.g.s. units. Notice that the slight mis-match of the coefficient with respect to Eq. (6.53) of Rybicki and Lightman (1979) is because we used C_γ instead of C_E.

If $\gamma(\nu) \ll \gamma_m \ll \gamma_M$, the corresponding frequency ν for $\gamma(\nu)$ is in the $F_\nu \propto \nu^{1/3}$ regime of the electron ensemble, one can replace $F(x)$ by its $\propto x^{1/3}$ asymptotic behavior (Eq. (5.6)), and then integrate over γ directly. This leads to (e.g. Wu et al. 2003, Exercise 5.2)

$$\begin{aligned}\alpha_\nu &= \frac{1}{2^{4/3}\Gamma\left(\frac{1}{3}\right)}\frac{(p+2)}{(p+\frac{2}{3})}\frac{e^3 B_\perp C_\gamma}{m_e^2 c^2}\left(\frac{4\pi m_e c}{3eB_\perp}\right)^{1/3}\gamma_m^{-(p+2/3)}\nu^{-5/3} \\ &\simeq 136\ \mathrm{cm}^{-1}\frac{(p+2)}{(p+\frac{2}{3})}C_\gamma B_\perp^{2/3}\gamma_m^{-(p+2/3)}\nu^{-5/3}\,. \end{aligned} \tag{5.40}$$

The numerical factor is for electrons in c.g.s. units.

The emission coefficient is (Rybicki and Lightman, 1979)

$$\begin{aligned} j_\nu &= \left(\frac{1}{4\pi}\right)\int_{\gamma_m}^{\gamma_M} P(\gamma,\nu)N(\gamma)d\gamma \\ &= \begin{cases} \frac{1}{2^{1/3}\Gamma\left(\frac{1}{3}\right)(p-\frac{1}{3})}\frac{e^3 B_\perp C_\gamma}{m_e c^2}\left(\frac{4\pi m_e c}{3eB_\perp}\right)^{1/3} & \\ \quad\times\gamma_m^{-(p-1/3)}\nu^{1/3}, & \gamma(\nu)\ll\gamma_m\ll\gamma_M, \\ \frac{2^{(p-1)/2}}{p+1}\frac{\sqrt{3}e^3 B_\perp C_\gamma}{4\pi m_e c^2}\left(\frac{4\pi m_e c}{3eB_\perp}\right)^{(1-p)/2} & \\ \quad\times\Gamma\left(\frac{3p+19}{12}\right)\Gamma\left(\frac{3p-1}{12}\right)\nu^{(1-p)/2}, & \gamma_m\ll\gamma(\nu)\ll\gamma_M. \end{cases} \end{aligned} \tag{5.41}$$

One can then derive the spectral indices in the synchrotron self-absorbed regime

$$F_\nu \propto S_\nu = \frac{j_\nu}{\alpha_\nu} \propto \begin{cases} \nu^{-(p-1)/2}/\nu^{-(p+4)/2} \propto \nu^{5/2}, & \gamma_m \ll \gamma(\nu) \ll \gamma_M, \\ \nu^{1/3}/\nu^{-5/3} \propto \nu^2, & \gamma(\nu) \ll \gamma_m \ll \gamma_M. \end{cases} \tag{5.42}$$

Self-Absorption Frequency (I): The Optical Depth Method

The self-absorption frequency ν_a, i.e. the frequency below which the synchrotron flux is self-absorbed, can be estimated in two different ways.

The first one is the *optical depth method*. The self-absorption frequency ν_a can be estimated by requiring

$$\tau_\nu = \int_{s_0}^{s} \alpha_\nu(\nu_a, s) ds = 1, \tag{5.43}$$

where s_0 and s are the locations of the emission point and the outer boundary towards observer of the emission region, respectively. Roughly speaking, one may assume that the emission region is uniform so that

$$\alpha_\nu(\nu_a)\Delta \sim 1, \tag{5.44}$$

where Δ is the characteristic width of the emission region.

There are several caveats for this approach. First, α_ν depends on the number density of the emitting electrons (through C_γ). Based on the *kinetic wind luminosity* L_w and the Lorentz factor Γ of the outflow "wind", one may estimate the total number of the electrons as $n_e \sim L_w/(4\pi R^2 \Gamma^2 m_p c^3)$, where R is the radius of the emission site from the central engine. However, this is based on the assumptions that the electrons are only those that are associated with protons – no additional electron–positron pairs exist – and that all the electrons are accelerated. In reality, not all these assumptions are necessarily satisfied. For example, there may be pairs generated in the emission site, and maybe only a small fraction of the electrons are accelerated. In the shock models, most electrons that contribute to the instantaneous spectrum are within a thin layer behind the shock front. Assuming a uniform distribution of the electrons in the entire shock region would introduce some uncertainties in deriving the self-absorption optical depth. Finally, since L_w is not an observable, one has to assume a direct connection between the observed photon luminosity L_γ and L_w (e.g. through a radiative efficiency parameter, $L_w = \eta_\gamma^{-1} L_\gamma$) to estimate n_e, and hence calculate ν_a.

Self-Absorption Frequency (II): The Blackbody Method

An alternative method to estimate ν_a is the *blackbody method*. Since the self-absorbed spectral regime for $\gamma(\nu) \ll \gamma_m \ll \gamma_M$ has an index 2, similar to the Rayleigh–Jeans regime of a blackbody spectrum, the self-absorption frequency may be derived as the intersection point between a blackbody (Rayleigh–Jeans) spectrum and the synchrotron spectrum, i.e.

$$I_\nu^{\rm bb}(\nu_a) \simeq 2kT\frac{\nu_a^2}{c^2} \simeq I_\nu^{\rm syn}(\nu_a), \tag{5.45}$$

where I_ν is the specific intensity. The temperature of the blackbody is taken as

$$\begin{aligned} kT &= \max(\gamma_m, \gamma_a) mc^2 \\ &= \begin{cases} \gamma_m mc^2, & \gamma_a \ll \gamma_m \ll \gamma_M, \\ \gamma_a mc^2, & \gamma_m \ll \gamma_a \ll \gamma_M. \end{cases} \end{aligned} \tag{5.46}$$

This method is widely used in the literature to estimate ν_a (e.g. Sari and Piran, 1999a; Kobayashi and Zhang, 2003b). The advantages of this method are that in most cases the derivations are straightforward, and that $I_\nu^{\rm syn}$ can be derived directly from the observations

so that the result does not depend on the unknown details of the GRB emission region (as encountered by the optical depth method).

One can prove that this method is consistent with the optical depth method (Shen and Zhang, 2009). The source function in the two spectral regimes can be derived from Eqs. (5.39), (5.40), and (5.41):

$$S_\nu = j_\nu/\alpha_\nu = \begin{cases} \frac{2(p+\frac{2}{3})}{(p+2)(p-\frac{1}{3})}\gamma_m m_e \nu^2, & \gamma(\nu) \ll \gamma_m \ll \gamma_M, \\ \frac{2m_e}{p+1}\left(\frac{2\pi m_e c}{3eB_\perp}\right)^{1/2} \frac{\Gamma\left(\frac{3p+19}{12}\right)\Gamma\left(\frac{3p-1}{12}\right)}{\Gamma\left(\frac{3p+22}{12}\right)\Gamma\left(\frac{3p+2}{12}\right)}\nu^{5/2}, & \gamma_m \ll \gamma(\nu) \ll \gamma_M. \end{cases} \tag{5.47}$$

Noting $\nu_a = (3/4\pi)\gamma_a^2(eB_\perp/m_e c)$, the specific intensity at ν_a can be generally expressed as

$$I_\nu(\nu_a) = \mathcal{C} \cdot 2kT\frac{\nu_a^2}{c^2}, \tag{5.48}$$

with kT defined in Eq. (5.46). The correction factor

$$\mathcal{C} = \begin{cases} \mathcal{C}_1(p) = \frac{(p+\frac{2}{3})}{(p+2)(p-\frac{1}{3})}, & \gamma_a \ll \gamma_m \ll \gamma_M, \\ \mathcal{C}_2(p) = \frac{1}{\sqrt{2}(p+1)}\frac{\Gamma\left(\frac{3p+19}{12}\right)\Gamma\left(\frac{3p-1}{12}\right)}{\Gamma\left(\frac{3p+22}{12}\right)\Gamma\left(\frac{3p+2}{12}\right)}, & \gamma_m \ll \gamma_a \ll \gamma_M, \end{cases} \tag{5.49}$$

is a function of p and is typically smaller than unity, e.g. $\mathcal{C}_1(2) = 0.4$, $\mathcal{C}_1(3) = 0.28$, $\mathcal{C}_2(2) = 0.32$, and $\mathcal{C}_2(3) = 0.19$. Compared with the blackbody method (Eq. (5.45)), the τ_ν method gives rise to a slightly lower value of ν_a.

5.1.7 Synchrotron Self-Absorption Heating

When synchrotron photons are absorbed by electrons, electrons are heated by the absorbed photons. Such a heating effect concerns electrons rather than photons, and can be quantified by a *synchrotron self-absorption cross section* (Ghisellini and Svensson, 1991):

$$\sigma_S(\gamma, \nu) = \begin{cases} \frac{1}{5}2^{2/3}\sqrt{3}\pi\Gamma^2(4/3)\frac{\sigma_T}{\alpha_f}\frac{B_q}{B}\left(\frac{\gamma\nu}{3\nu_L}\right)^{-5/3}, & \frac{\nu_L}{\gamma} < \nu \ll \frac{3}{2}\gamma^2\nu_L, \\ \frac{\sqrt{3}}{2}\pi^2\frac{\sigma_T}{\alpha_f}\frac{B_q}{B}\frac{1}{\gamma^3}\left(\frac{\nu_L}{\nu}\right)\exp\left(\frac{-2\nu}{3\gamma^2\nu_L}\right), & \nu \gg \frac{3}{2}\gamma^2\nu_L, \end{cases} \tag{5.50}$$

where

$$\alpha_f \equiv \frac{e^2}{\hbar c} \simeq \frac{1}{137} \tag{5.51}$$

is the fine structure constant,

$$B_q = \frac{m_e^2 c^3}{\hbar e} \simeq 4.414 \times 10^{13}\ \mathrm{G} \tag{5.52}$$

is the critical magnetic field strength (defined by equating electron rest mass energy and the gyration energy, i.e. $m_e c^2 = \hbar(eB/m_e c)$), and $\nu_L = eB/2\pi m_e c$ is the electron cyclotron frequency. This cross section is derived from the synchrotron self-absorption coefficient

through 3-level Einstein coefficients and relations (Ghisellini and Svensson, 1991), and describes the cross section of an electron with Lorentz factor γ absorbing a photon with frequency ν.

One important implication for synchrotron heating is that, if

$$\gamma_a > \gamma_c, \tag{5.53}$$

the electrons that are supposed to cool down are heated by synchrotron self-absorption, so that they *pile up* at a characteristic energy close to γ_a (Ghisellini et al., 1988). We define this regime as the *strong absorption* regime. The opposite

$$\gamma_a < \gamma_c \tag{5.54}$$

regime is defined as the *weak absorption* regime, in which synchrotron self-absorption heating is not important.

In the strong absorption regime, the electron pile-up condition may be derived as follows (Gao et al., 2013c). One may take an approximate form of the self-absorption heating cross section:

$$\sigma_S(\gamma,\nu)=\begin{cases}\frac{1}{5}2^{2/3}\sqrt{3}\pi\Gamma^2(4/3)\frac{\sigma_{\rm T}}{\alpha_{\rm f}}\frac{B_q}{B}\left(\frac{\gamma\nu}{3\nu_{\rm L}}\right)^{-5/3}, & \frac{\nu_{\rm L}}{\gamma}<\nu\le\frac{3}{2}\gamma^2\nu_{\rm L},\\ 0, & \nu>\frac{3}{2}\gamma^2\nu_{\rm L}.\end{cases} \tag{5.55}$$

For an electron with Lorentz factor γ, the heating rate due to synchrotron self-absorption may be estimated as

$$\dot{\gamma}^{+}(\gamma)=\int_0^\infty cn_\nu(\gamma)h\nu\sigma_{\rm S}(\gamma,\nu)d\nu, \tag{5.56}$$

where $n_\nu(\gamma)$ is the specific photon number density at frequency ν contributed by an electron with Lorentz factor γ.

The cooling rate of an electron with Lorentz factor γ due to synchrotron and also synchrotron self-Compton (SSC, see §5.2.3 below) is

$$\dot{\gamma}^{-}(\gamma)=(1+Y)P_{\rm syn}=(1+Y)\frac{4}{3}\sigma_{\rm T}c\gamma^2\frac{B^2}{8\pi}, \tag{5.57}$$

where $Y\equiv\frac{P_{\rm SSC}}{P_{\rm syn}}$ is a parameter defined in Eq. (5.100) in §5.2.3, which describes the relative importance between synchrotron self-Compton and synchrotron processes.

By balancing the heating and cooling rate, one can derive a critical Lorentz factor at which electrons pile up:

$$\dot{\gamma}^{+}(\gamma_{\rm pile\text{-}up})=\dot{\gamma}^{-}(\gamma_{\rm pile\text{-}up}). \tag{5.58}$$

The shape of the energy distribution of electrons around $\gamma_{\rm pile\text{-}up}$ is close to a relativistic Maxwellian. Notice that such a pile-up condition is only valid when $\gamma_a > \gamma_c$, with $\gamma_{\rm pile\text{-}up} \sim \gamma_a$. In the weak absorption regime ($\gamma_a < \gamma_c$), self-absorption heating is not important, so no pile-up is expected.

Within the GRB context, the strong absorption regime may occur only in rare situations. One application may be the reverse shock emission in a dense wind medium (Kobayashi et al., 2004; Gao et al., 2013c).

5.1.8 Broken Power-Law Spectra

To summarize, the synchrotron radiation spectrum of an ensemble of electrons with a continuously injected, power-law distributed source function, which undergo synchrotron cooling and synchrotron self-absorption, can be expressed in the form a multi-segment broken power law.

Before writing down the expressions of the observed flux spectra, let us clarify that the above analyses are within the rest frame where electrons have a random distribution in direction. This is the *comoving* frame of the shocks in the GRB problem. In the observer frame, the entire spectrum is Doppler-boosted due to the bulk motion of the ejecta. This systematically changes the break frequencies in the broken power-law spectra, i.e. $\nu_{\rm ch} = \mathcal{D}\nu'_{\rm ch} \simeq \Gamma\nu'_{\rm ch}$. The spectral indices in different spectral regimes, on the other hand, remain unchanged.

Inspecting Eq. (5.1), one can derive the average *peak specific emission power* of an individual electron in the observer frame (Wijers and Galama, 1999):

$$P_{\nu,\rm max} = \frac{\sqrt{3}\phi e^3}{m_e c^2} B\Gamma, \tag{5.59}$$

where ϕ is a factor of order unity that combines the maximum value of $F(x)$ and the average of the angles. The Lorentz factor Γ comes from the relativistic correction: in the observer frame, the total emission power (dE/dt) is larger by a factor of $\sim \Gamma^2$ ($dE \simeq \Gamma dE'$, $dt \simeq \Gamma^{-1}dt'$), and the typical frequency is larger by a factor of Γ ($\nu_{\rm ch} \simeq \Gamma\nu'_{\rm ch}$). Notice that this specific emission power Eq. (5.59) does not depend on the electron energy γ, so that electrons with different energies share the same value (but the characteristic frequencies are different).

The flux density at a particular frequency is therefore only proportional to the number of electrons that contribute to that frequency. For a power-law distribution (Eq. (5.12)), the peak flux density is proportional to the number of electrons that have the lowest energy (γ_m for slow cooling and γ_c for fast cooling), e.g. $N(\gamma_m)\Delta\gamma_m = [C_\gamma/\gamma_m^{(p-1)}](\Delta\gamma_m/\gamma_m)$ for slow cooling. This is essentially the total (energy integrated) number of electrons, $N_{\rm tot} \simeq [C_\gamma/\gamma_m^{(p-1)}](p-1)^{-1}$, as long as $p > 1$ is satisfied. In practice, usually one writes

$$F_{\nu,\rm max} = (1+z)\frac{N_{\rm tot}P_{\nu,\rm max}}{4\pi D_{\rm L}^2}, \tag{5.60}$$

where z is the redshift of the burst,

$$D_{\rm L} = (1+z)\frac{c}{H_0}\int_0^z \frac{dz'}{\sqrt{\Omega_m(1+z')^3+\Omega_\Lambda}} \tag{5.61}$$

is the luminosity distance of the burst (see also Eq. (2.40)), H_0 is the Hubble constant, and Ω_m and Ω_Λ are the energy density parameters for matter and dark energy, respectively.

There are altogether six different orderings among ν_a, ν_m, and ν_c. One may classify them in two different ways. One way is based on the relative ordering between ν_m and ν_c, i.e. slow cooling for $\nu_m < \nu_c$ and fast cooling for $\nu_c < \nu_m$. The other way is based on the relative ordering between ν_a and ν_c, i.e. $\nu_a < \nu_c$ for weak absorption and $\nu_a > \nu_c$ for

strong absorption (see details in §5.1.7). In the following, we order the six spectral regimes based on the second approach, i.e. weak absorption for (I–III), and strong absorption for (IV–VI). The slow cooling cases are (I), (II), and (V), whereas the fast cooling cases are (III), (IV), and (VI). For the strong absorption cases, we adopt an approximate broken power-law form with an abrupt jump around the pile-up frequency, with a caution that the real spectrum should show a smooth bump, the shape of which depends on electron energy distribution near $\gamma_{\rm pile\text{-}up}$. The indicative broken power-law spectra of the six cases are displayed in Fig. 5.4 (Exercise 5.3).

The three weak absorption cases are summarized below. Regimes (I) and (III) were published by Sari et al. (1998), and regime (II) was published by, e.g. Dermer et al. (2000b).

(I) $\nu_a < \nu_m < \nu_c < \nu_M$ (slow cooling, weak absorption):

$$F_\nu = F_{\nu,\max}\begin{cases}\left(\frac{\nu_a}{\nu_m}\right)^{\frac{1}{3}}\left(\frac{\nu}{\nu_a}\right)^2, & \nu \le \nu_a,\\ \left(\frac{\nu}{\nu_m}\right)^{\frac{1}{3}}, & \nu_a < \nu \le \nu_m,\\ \left(\frac{\nu}{\nu_m}\right)^{-\frac{p-1}{2}}, & \nu_m < \nu \le \nu_c,\\ \left(\frac{\nu_c}{\nu_m}\right)^{-\frac{p-1}{2}}\left(\frac{\nu}{\nu_c}\right)^{-\frac{p}{2}}, & \nu_c < \nu \le \nu_M.\end{cases} \tag{5.62}$$

(II) $\nu_m < \nu_a < \nu_c < \nu_M$ (slow cooling, weak absorption):

$$F_\nu = F_{\nu,\max}\begin{cases}\left(\frac{\nu_a}{\nu_m}\right)^{-\frac{p-1}{2}}\left(\frac{\nu_m}{\nu_a}\right)^{\frac{5}{2}}\left(\frac{\nu}{\nu_m}\right)^2 = \left(\frac{\nu_m}{\nu_a}\right)^{\frac{p+4}{2}}\left(\frac{\nu}{\nu_m}\right)^2, & \nu \le \nu_m,\\ \left(\frac{\nu_a}{\nu_m}\right)^{-\frac{p-1}{2}}\left(\frac{\nu}{\nu_a}\right)^{\frac{5}{2}}, & \nu_m < \nu \le \nu_a,\\ \left(\frac{\nu}{\nu_m}\right)^{-\frac{p-1}{2}}, & \nu_a < \nu \le \nu_c,\\ \left(\frac{\nu_c}{\nu_m}\right)^{-\frac{p-1}{2}}\left(\frac{\nu}{\nu_c}\right)^{-\frac{p}{2}}, & \nu_c < \nu \le \nu_M.\end{cases} \tag{5.63}$$

(III) $\nu_a < \nu_c < \nu_m < \nu_M$ (fast cooling, weak absorption):

$$F_\nu = F_{\nu,\max}\begin{cases}\left(\frac{\nu_a}{\nu_c}\right)^{\frac{1}{3}}\left(\frac{\nu}{\nu_a}\right)^2, & \nu \le \nu_a,\\ \left(\frac{\nu}{\nu_c}\right)^{\frac{1}{3}}, & \nu_a < \nu \le \nu_c,\\ \left(\frac{\nu}{\nu_c}\right)^{-\frac{1}{2}}, & \nu_c < \nu \le \nu_m,\\ \left(\frac{\nu_m}{\nu_c}\right)^{-\frac{1}{2}}\left(\frac{\nu}{\nu_m}\right)^{-\frac{p}{2}}, & \nu_m < \nu \le \nu_M.\end{cases} \tag{5.64}$$

For the three strong absorption cases, we adopt the following approximate treatment following Gao et al. (2013c). For the quasi-thermal electron component, we take $N(\gamma) \propto \gamma^2$ for $\gamma < \gamma_a$, and a sharp cutoff above γ_a. In reality, the transition around the thermal peak should be smooth. This approximate treatment nonetheless catches the asymptotic power-law behaviors at $\gamma \gg \gamma_a$ and $\gamma \ll \gamma_a$.

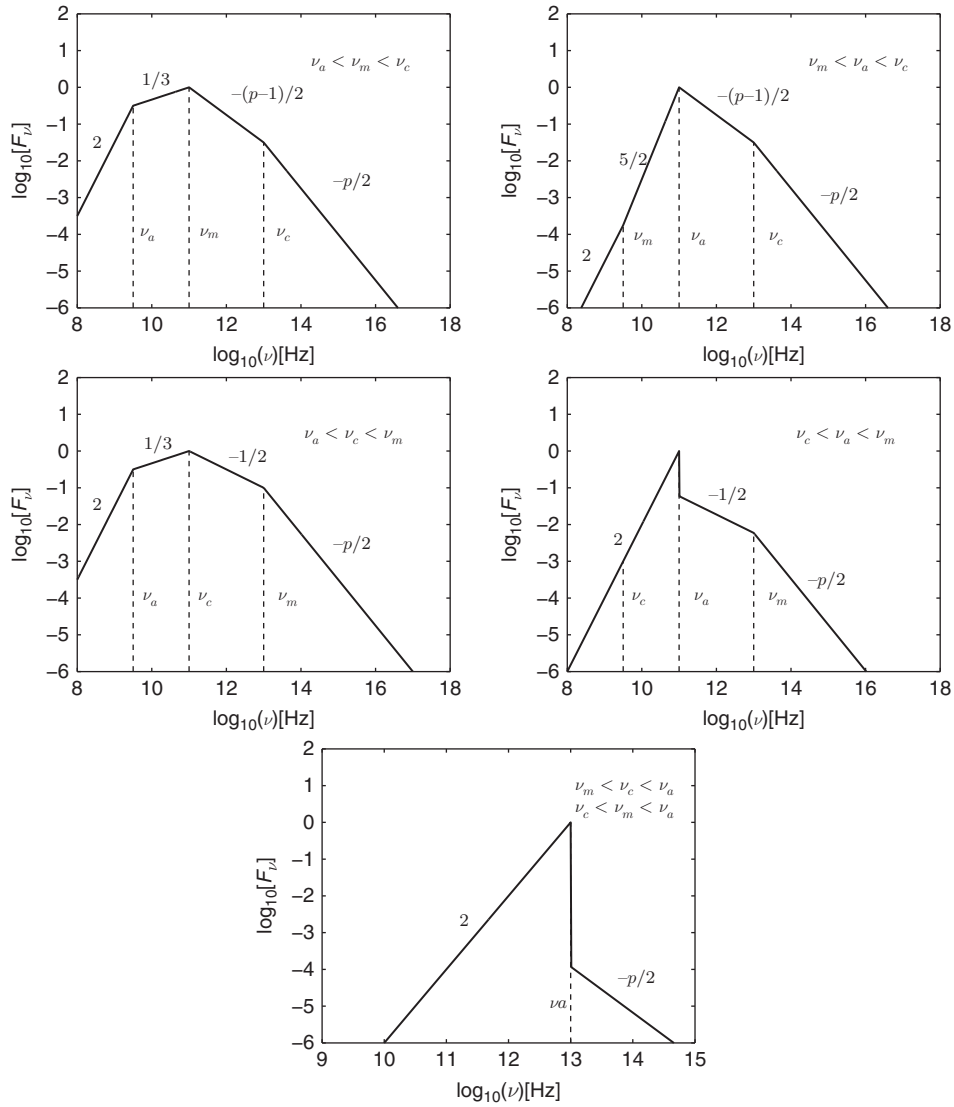

Figure 5.4 Synchrotron spectra of electrons with different orders of ν_a, ν_m, and ν_c. The first four panels are, respectively, from top left to bottom right: (I) $\nu_a < \nu_m < \nu_c$; (II) $\nu_m < \nu_a < \nu_c$; (III) $\nu_a < \nu_c < \nu_m$; (IV) $\nu_c < \nu_a < \nu_m$. The last panel applies for both regimes (V) and (VI): $\nu_a > \max(\nu_m, \nu_c)$. For strong absorption (electron pile-up) cases (VI–VI), a very rough approximation of the pile-up spectra is adopted to allow a power-law description of the spectra. See text for details. Figure courtesy He Gao.

(IV) $\nu_c < \nu_a < \nu_m < \nu_M$ (fast cooling, strong absorption):

$$F_\nu = F_{\nu,\max} \begin{cases} \left(\frac{\nu}{\nu_a}\right)^2, & \nu \le \nu_a, \\ \mathcal{R}\left(\frac{\nu}{\nu_a}\right)^{-\frac{1}{2}}, & \nu_a < \nu \le \nu_m, \\ \mathcal{R}\left(\frac{\nu_m}{\nu_a}\right)^{-\frac{1}{2}}\left(\frac{\nu}{\nu_m}\right)^{-\frac{p}{2}}, & \nu_m < \nu \le \nu_M, \end{cases}$$

where

$$\mathcal{R} = \frac{\gamma_c}{3\gamma_a} \tag{5.65}$$

is the flux ratio between the pile-up peak and the optically thin limit at ν_a.

(V) and (VI) $\max(\nu_m, \nu_c) < \nu_a < \nu_M$:

It turns out that the regimes (V) and (VI) have the same spectral form. As long as ν_a is above both ν_m and ν_c, the ordering between ν_m and ν_c no longer matters, since electrons are piled up around $\gamma_{\rm pile\text{-}up}$, and the electron population below $\gamma_{\rm pile\text{-}up}$ is essentially thermalized. In these two regimes, one has

$$F_\nu = F_{\nu,\max} \begin{cases} \left(\frac{\nu}{\nu_a}\right)^2, & \nu \le \nu_a, \\ \mathcal{R}\left(\frac{\nu}{\nu_a}\right)^{-\frac{p}{2}}, & \nu_a < \nu < \nu_M, \end{cases}$$

where the flux ratio between the pile-up peak and the optically thin limit at ν_a is

$$\mathcal{R} = (p-1)\frac{\gamma_c}{3\gamma_a}\left(\frac{\gamma_m}{\gamma_a}\right)^{p-1} \tag{5.66}$$

for $\nu_m < \nu_c < \nu_a < \nu_M$ (regime V), and

$$\mathcal{R} = \frac{\gamma_{\rm c}}{3\gamma_{\rm a}}\left(\frac{\gamma_m}{\gamma_{\rm a}}\right)^{p-1} \tag{5.67}$$

for $\nu_c < \nu_m < \nu_a < \nu_M$ (regime VI).

In most GRB problems, ν_a is not high enough to enter the strong absorption regime. The most common cases are (I) and (III). Nonetheless, other regimes may become relevant for the blastwave models invoking a dense circumburst medium (e.g. a wind medium), since in these cases self-absorption becomes more important, and ν_a can exceed ν_m or ν_c, or even both.

5.1.9 Synchrotron Polarization

Synchrotron emission from one electron is elliptically polarized. At angular frequency ω, the perpendicular and parallel components (with respect to the magnetic field direction in the plane perpendicular to the propagation direction of the electromagnetic wave) of the specific power are (Rybicki and Lightman, 1979)

$$P_\perp(\omega) = \frac{\sqrt{3}e^3 B_\perp}{4\pi mc^2}[F(x) + G(x)], \tag{5.68}$$

$$P_\parallel(\omega) = \frac{\sqrt{3}e^3 B_\perp}{4\pi mc^2}[F(x) - G(x)], \tag{5.69}$$

where

$$F(x) \equiv x\int_x^\infty K_{\frac{5}{3}}(\xi)d\xi, \tag{5.70}$$

$$G(x) \equiv xK_{\frac{2}{3}}(x), \tag{5.71}$$

and $x \equiv \omega/\omega_{\rm ch} = \nu/\nu_{\rm ch}$. The polarization degree of one single electron at frequency ω is

$$\Pi(\omega) = \frac{P_\perp(\omega) - P_\parallel(\omega)}{P_\perp(\omega) + P_\parallel(\omega)} = \frac{G(x)}{F(x)}. \tag{5.72}$$

This polarization degree is typically high. The polarization degree of the frequency integrated radiation is

$$\Pi = \frac{\int G(x)dx}{\int F(x)dx} = 75\%. \tag{5.73}$$

For a power-law distribution of electrons ($N(\gamma)d\gamma \propto \gamma^{-p}d\gamma$), the linear polarization degree is

$$\Pi = \frac{G(x)\gamma^{-p}d\gamma}{F(x)\gamma^{-p}d\gamma} = \frac{G(x)x^{(p-3)/2}dx}{F(x)x^{(p-3)/2}dx} = \frac{p+1}{p+7/3}, \tag{5.74}$$

where $\gamma \propto x^{-1/2}$, and the property of the Γ function, $\Gamma(q+1) = q\Gamma(q)$, has been used. For $p = 3$, Eq. (5.74) gives 75%, same as Eq. (5.73).

For synchrotron emission in a random magnetic field, the polarizations are cancelled out, so that the net polarization degree is 0. In an ordered magnetic field, synchrotron emission has strong linear polarization, with a polarization degree defined by (5.74). For $p = 2.5$, this is $\Pi \sim 72\%$.

5.2 Inverse Compton Scattering

Besides synchrotron radiation, another important radiation mechanism in GRBs is inverse Compton scattering of electrons off seed photons in the emission region.

5.2.1 Basics

Concepts

We first review several concepts regarding interactions between electrons and photons (Rybicki and Lightman, 1979).

Consider an electron at rest and a photon with frequency ν interacting with the electron. After the interaction, a photon with frequency ν_1 is released in a direction θ with respect to the initial direction. Energy and momentum conservation immediately gives

$$h\nu_1 = \frac{h\nu}{1 + \frac{h\nu}{m_e c^2}(1 - \cos\theta)}. \tag{5.75}$$

If $h\nu \ll m_e c^2$, one has

$$h\nu_1 \sim h\nu. \tag{5.76}$$

This is called *Thomson scattering*. The net result is that the electron scatters the incoming photon to a random direction. If, however, $h\nu/m_e c^2$ is not negligible, one has $h\nu_1 < h\nu$, and the electron receives a "kick" from the photon. This is *Compton scattering*.

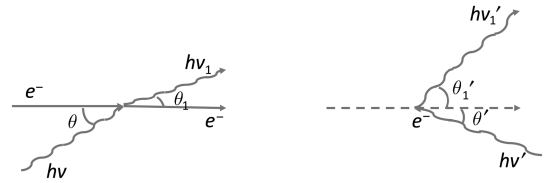

Figure 5.5 An IC process viewed in the lab frame (*left*) and in the electron rest frame (*right*).

Now consider an electron moving with a relativistic speed (with Lorentz factor γ), and scattering off a photon with frequency ν (Fig. 5.5 left). This is *inverse Compton (IC) scattering*. The incident photon can come from any direction (θ is arbitrary), but after the scattering, the photon direction is close to the direction of electron motion (small θ_1). In the rest frame of the electron (Fig. 5.5 right), the incident photon comes from a small angle (small θ'), but the scattered photon goes in a random direction (arbitrary θ_1'). If $h\nu' \ll m_e c^2$ is satisfied, then the IC is in the *Thomson regime*, i.e. $\nu_1' \simeq \nu'$. Otherwise, the IC is in the *Klein–Nishina regime*.

An IC process transfers energy from the moving electron to the photon. Roughly speaking, one has

$$h\nu : h\nu' : h\nu_1' : h\nu_1 \sim 1 : \gamma : \gamma : \gamma^2 \tag{5.77}$$

in the Thomson regime. This can be proved as follows.

According to the Doppler transformation formula, one has

$$h\nu = \mathcal{D} h\nu' = \frac{1}{\gamma(1-\beta\cos\theta)h\nu'}, \tag{5.78}$$

$$h\nu_1 = \mathcal{D}_1 h\nu_1' = \gamma(1+\beta\cos\theta_1')h\nu_1'. \tag{5.79}$$

In the Thomson regime:

$$h\nu_1' \simeq h\nu', \tag{5.80}$$

so

$$h\nu_1 \simeq \gamma(1+\beta\cos\theta_1')\gamma(1-\beta\cos\theta)\cdot h\nu \sim \gamma^2 h\nu, \tag{5.81}$$

since generally both θ_1' and θ are not close to 0 (Fig. 5.5).

In the Klein–Nishina regime, one has

$$h\nu_1' < h\nu', \tag{5.82}$$

since the electron receives a recoil force. The energy of the scattered photon in the electron rest frame is at most the electron rest mass energy

$$h\nu_1' \lesssim m_e c^2, \quad h\nu_1 \lesssim \gamma m_e c^2. \tag{5.83}$$

Overall one has

$$h\nu_1 \sim \min(\gamma^2 h\nu, \gamma m_e c^2) \tag{5.84}$$

in the lab frame.

Cross Section

In the Thomson regime, the scattering cross section is defined by the *Thomson cross section* (Rybicki and Lightman, 1979):

$$\sigma_{\rm T} \equiv \frac{8\pi}{3} r_0^2, \tag{5.85}$$

where

$$r_0 = \frac{e^2}{m_e c^2} \tag{5.86}$$

is the classical radius of the electron.

More generally, the *Compton scattering cross section* can be written as (Rybicki and Lightman, 1979)

$$\begin{aligned}\sigma &= \frac{3}{4}\sigma_{\rm T}\left[\frac{1+x}{x^3}\left\{\frac{2x(1+x)}{1+2x} - \ln(1+2x)\right\} + \frac{1}{2x}\ln(1+2x) - \frac{1+3x}{(1+2x)^2}\right] \\ &= \begin{cases} \sigma_{\rm T}(1-2x+\frac{26}{5}x^2+\cdots), & x \ll 1, \\ \frac{3}{8}\sigma_{\rm T} x^{-1}(\ln 2x + \frac{1}{2}), & x \gg 1, \end{cases}\end{aligned} \tag{5.87}$$

where

$$x \equiv \frac{h\nu}{m_e c^2}. \tag{5.88}$$

One can see that $\sigma \sim \sigma_{\rm T}$ in the Thomson regime ($x \ll 1$), and σ is greatly suppressed ($\propto \sigma_{\rm T}/x$) in the Klein–Nishina regime ($x \gg 1$).

IC Emission Power

In the Thomson regime, the IC *emission power* of a single electron takes the form (Rybicki and Lightman, 1979)

$$P_{\rm IC} \simeq \frac{4}{3}\gamma^2 \sigma_{\rm T} c \beta^2 U_{\rm ph}, \tag{5.89}$$

where $U_{\rm ph}$ is the energy density of the target photons. Recall that the synchrotron power of a single particle takes the form

$$P_{\rm syn} = \frac{4}{3}\gamma^2 \sigma_{\rm T} c \beta^2 U_B, \tag{5.90}$$

where U_B is the energy density of the magnetic fields; one then has

$$\frac{P_{\rm IC}}{P_{\rm syn}} \simeq \frac{U_{\rm ph}}{U_B}. \tag{5.91}$$

The relative importance between the two energy densities therefore decides which mechanism is the dominant cooling mechanism for electrons.

5.2.2 Single Inverse Compton Scattering

Whether a photon is scattered once or multiple times depends on the *Thomson optical depth* for electron scattering, which is the optical depth of electrons seen by a photon:

$$\tau_{\rm es} = \sigma_{\rm T} n_e \Delta = \sigma_{\rm T} n'_e \Delta', \tag{5.92}$$

where Δ (Δ') is the characteristic width of the emission region in the lab (comoving) frame, and n_e (n'_e) is the electron number density in the lab (comoving) frame. In the GRB problem, $\tau = 1$ defines the *photosphere* of the ejecta below which photons are opaque and undergo multiple scatterings before escaping. In the regions well above the photosphere, e.g. the optically thin internal shocks, magnetic dissipation sites, as well as the blastwave region where afterglow photons are emitted, one has $\tau \ll 1$, so that *single scattering* is relevant. We first discuss the IC spectrum in this regime.

Since IC emission invokes both electrons and seed photons, an IC spectrum depends on both the incident photon spectrum and the energy distribution of electrons.

Isotropic, Mono-energetic Photons vs. Mono-energetic Electrons

The simplest case invokes a mono-energetic photon field scattered off electrons with a given energy $\gamma m_e c^2$, with both photons and electrons having an isotropic distribution.

Denoting the emission intensity of the isotropic incident photon field as

$$I(\epsilon) = F_0 \delta(\epsilon - \epsilon_0), \tag{5.93}$$

one can derive the IC spectrum in the lab frame (Rybicki and Lightman, 1979):

$$j(\epsilon_1) = \frac{3N\sigma_{\rm T} F_0}{4\gamma^3 \epsilon_0} f(x), \tag{5.94}$$

where

$$f(x) = 1 + x + 2x\ln x - 2x^2, \;\; 0 < x < 1, \tag{5.95}$$

and

$$x \equiv \frac{\epsilon_1}{4\gamma^2 \epsilon_0} = \frac{\nu_1}{4\gamma^2 \nu_0}. \tag{5.96}$$

One can see that there is a maximum value of the scattered photon energy $\nu_{1,\rm max} = 4\gamma^2 \nu_0$. This is defined by the kinetic constraint $\nu_1/\nu_0 < (1+\beta)/(1-\beta)$, which $\simeq 4\gamma^2$ when $\beta \sim 1$ ($\gamma \gg 1$).

IC Spectrum: Power-Law Distribution of Electrons

Usually a more relevant case is to invoke a power-law distribution of electrons (Eq. (5.12)):

$$N(\gamma) d\gamma = C_\gamma \gamma^{-p} d\gamma. \tag{5.97}$$

Let us denote the specific photon number density $n_\nu d\nu$ without specifying its form, the IC volume emissivity can be expressed as (Rybicki and Lightman, 1979; Sari and Esin, 2001)

$$\begin{aligned} j_{\nu_1}^{\rm IC} &= \frac{dE}{dVd\nu_1 dt} \\ &= 3\sigma_{\rm T}\int_{\gamma_m}^{\infty} d\gamma N(\gamma)\int_0^1 dx f(x) n_\nu(x) \\ &= (3/8)\sigma_{\rm T} c C_\gamma A(p)\nu_1^{-(p-1)/2}\int d\nu \nu^{(p-1)/2} n_\nu(\nu) \\ &\propto \nu_1^{-(p-1)/2}, \end{aligned} \tag{5.98}$$

where

$$A(p) = \frac{2^{p+3}(p^2+4p+11)}{(p+3)^2(p+5)(p+1)}. \tag{5.99}$$

So the spectrum is again a power law with index $-(p-1)/2$ (similar to synchrotron radiation), regardless of the detailed spectrum of the incident photons.

5.2.3 Synchrotron Self-Compton (SSC) and Enhanced Cooling

The most commonly discussed IC process is synchrotron self-Compton (SSC). This process is important, since it is always associated with synchrotron radiation. The bottom line is that synchrotron photons produced by electrons in an emission region will also be upscattered by the same group of electrons. In principle, the SSC photons can be upscattered again. So, more generally, one may define the SSC emission as the first-order SSC, keeping in mind that there should be second-, third-, ... order SSC components as well. In reality, the higher order SSC processes would be significantly suppressed by the Klein–Nishina effect (recall that the cross section of Compton scattering in the Klein–Nishina regime decreases linearly with the energy of the incident photons, Eq. (5.87) in the $x \gg 1$ regime). Usually one deals with at most the second-order SSC in GRB problems.

Enhanced Cooling

Since electrons radiate synchrotron photons, and in the meantime upscatter synchrotron photons, they lose energy more efficiently than via synchrotron radiation alone. In view of the similar expressions of the synchrotron and IC emission powers (Eqs. (5.90) and (5.89)), it is convenient to define[2]

$$Y \equiv \frac{P_{\rm IC}}{P_{\rm syn}} \simeq \frac{U_{\rm syn}}{U_B}, \tag{5.100}$$

where $U_{\rm syn}$ is the energy density of the synchrotron photons.

The second part of the equation is valid when IC is in the Thomson regime. Notice that in principle Y is γ-dependent. In the Thomson regime, both $P_{\rm IC}$ and $P_{\rm syn}$ are proportional to γ^2 and cancel out in the expression for Y.

[2] This Y parameter is not always identical to the Compton y parameter defined by Rybicki and Lightman (1979), which describes how efficiently a photon changes its energy during propagation. See §5.2.5 for detailed discussion.

Considering higher order SSC processes, in general one can define

$$Y_1 = Y = \frac{P_{\rm SSC,1}}{P_{\rm syn}} \simeq \frac{U_{\rm syn}}{U_B}, \tag{5.101}$$

$$Y_2 = \frac{P_{\rm SSC,2}}{P_{\rm SSC,1}} \simeq \frac{U_{\rm SSC,1}}{U_{\rm syn}}, \tag{5.102}$$

$$\vdots$$

where $U_{\rm SSC,1}$ is the energy density of the photons produced in the first-order SSC process, etc. Here the second part of the equations is again only valid in the Thomson regime. The total emission power of the electron can be written as

$$\begin{aligned} P_{\rm tot} &= P_{\rm syn} + P_{\rm SSC,1} + P_{\rm SSC,2} + \cdots \\ &\simeq \frac{4}{3}\gamma^2 \sigma_{\rm T} c \beta^2 U_B (1 + Y_1 + Y_1 Y_2 + \cdots) \\ &= P_{\rm syn}(1 + Y_1 + Y_1 Y_2 + \cdots). \end{aligned} \tag{5.103}$$

So cooling is enhanced by a factor of $(1+Y_1+Y_1Y_2+\cdots)$. If the Klein–Nishina correction is not important, one will have $Y_1 = Y_2 = \cdots = Y$. This is because a first-order SSC power that is Y times the synchrotron power will produce a SSC photon energy density that is also Y times that of the synchrotron. So the higher order SSC terms become progressively important (unimportant) if $Y > 1$ ($Y < 1$). In particular, for $Y > 1$, one will suffer a divergence problem in energy (Derishev et al., 2001; Piran et al., 2009). For example, one model for interpreting prompt emission of the "naked-eye" GRB (GRB 080319B) attributed the observed prompt optical emission as the synchrotron radiation component, while the observed γ-ray emission as the first-order SSC component (e.g. Racusin et al., 2008; Kumar and Panaitescu, 2008). If this is the case, the second-order SSC will not be in the Klein–Nishina regime. Since the observations give $Y \sim 10$, one drawback of such a model is to demand a much larger energy budget than observed, with 10 times more energy released in the >100 GeV energy band.

In most GRB problems (e.g. afterglow emission, and prompt emission if the sub-MeV γ-rays are attributed to synchrotron radiation), usually the second-order SSC component is not important. One therefore has

$$P_{\rm tot} = P_{\rm syn}(1 + Y). \tag{5.104}$$

If the Klein–Nishina effect is already important at the first-order SSC, one needs to introduce a correction factor $Y_{\rm KN} < 1$ to Y, so that

$$Y(\gamma) = \frac{U_{\rm syn}}{U_B} Y_{\rm KN}(\gamma), \tag{5.105}$$

where

$$Y_{\rm KN}(\gamma) \sim \min\left[1, \left(\frac{\Gamma mc^2}{\gamma h \nu_{\rm syn}}\right)^2\right]. \tag{5.106}$$

Here Γ is the bulk Lorentz factor of the outflow, γ is the electron Lorentz factor in the comoving frame, and $\nu_{\rm syn}$ is the νF_ν peak synchrotron frequency in the observer's frame. The factor $(\Gamma mc^2/\gamma h\nu_{\rm syn})$ is the ratio between the electron rest mass energy mc^2 and the seed photon energy seen in the electron's rest frame, $\gamma(h\nu_{\rm syn})/\Gamma$. This factor is corrected

twice, once through the characteristic SSC frequency and then through the scattering optical depth due to the decrease of the KN cross section, so that it has a second power in Eq. (5.106).

If the Klein–Nishina effect is not important for the first-order SSC, but contributes in a higher order SSC component (e.g. second-order SSC), a $Y_{\rm KN}(\gamma)$ factor should be introduced to the corresponding Y value of the relevant order of the SSC component, with the frequency $\nu_{\rm syn}$ in Eq. (5.106) replaced by the corresponding typical seed photon frequency.

More generally, if the emission region is permeated with other photons not of synchrotron origin, the electrons would also upscatter these photons and lose energy. For example, in the internal shock region, thermal photons from the photosphere may pass through and tap the energy of the electrons by scattering off them. In the early afterglow phase, electrons in the external shock region may be cooled by photons produced from the prompt emission region or early X-ray flares. One may generally define these processes as *external IC* (EIC). Similar to the SSC process, one may define

$$Y_{\rm EIC,1} = \frac{P_{\rm EIC,1}}{P_{\rm syn}} = \frac{U_{\rm E-ph}}{U_B}, \tag{5.107}$$

$$Y_{\rm EIC,2} = \frac{P_{\rm EIC,2}}{P_{\rm EIC,1}} = \frac{U_{\rm EIC,1}}{U_{\rm E-ph}}, \tag{5.108}$$

$$\vdots$$

where $U_{\rm E-ph}$ is the external photon energy density in the emission region, $U_{\rm EIC,1}$ is the first-order EIC photon energy density, etc., and the Thomson regime is assumed. Putting everything together, one therefore has

$$P_{\rm tot} = P_{\rm syn}(1+\tilde{Y}), \tag{5.109}$$

where

$$\tilde{Y} = (1 + Y_1 + Y_1 Y_2 + \cdots + Y_{\rm EIC,1} + Y_{\rm EIC,1} Y_{\rm EIC,2} + \cdots) \tag{5.110}$$

is the effective Y parameter.

All these processes enhance electron cooling. At any epoch t, the electron cooling Lorentz factor is smaller by a factor of $(1+\tilde{Y})$, i.e.

$$\gamma_c = \frac{6\pi mc}{\sigma_{\rm T} B^2 t (1+\tilde{Y})}. \tag{5.111}$$

Y Parameter

The Y parameter can be connected to shock microphysics parameters for SSC processes. Let us adopt the parameterization of ϵ_e and ϵ_B as the fractions of shock internal energy that is distributed to electrons and magnetic fields, respectively. One can derive the Y parameters as follows (Exercise 5.4).

We first consider the simplest case with first-order SSC only, following Sari and Esin (2001). From the definition of Y, the synchrotron photon energy density is a factor $1/(1+Y)$ of the total emission energy of electrons (the other fraction $Y/(1+Y)$ goes to SSC). One therefore has

$$Y \equiv \frac{L_{\rm SSC}}{L_{\rm syn}} = \frac{U_{\rm syn}}{U_B} = \frac{\eta_e U_e/(1+Y)}{U_B} = \frac{\eta_e \epsilon_e}{\epsilon_B (1+Y)}, \tag{5.112}$$

where

$$\eta_e = \begin{cases} 1, & \text{fast cooling,} \\ \left(\frac{\gamma_c}{\gamma_m}\right)^{2-p}, & \text{slow cooling,} \end{cases} \tag{5.113}$$

is the electron radiation efficiency. Solving the equation

$$\epsilon_B Y^2 + \epsilon_B Y - \eta_e \epsilon_e = 0, \tag{5.114}$$

one gets

$$Y = \frac{-1+\sqrt{1+4\eta_e \epsilon_e/\epsilon_B}}{2} = \begin{cases} \frac{\eta_e \epsilon_e}{\epsilon_B}, & \frac{\eta_e \epsilon_e}{\epsilon_B} \ll 1, \\ \left(\frac{\eta_e \epsilon_e}{\epsilon_B}\right)^{1/2}, & \frac{\eta_e \epsilon_e}{\epsilon_B} \gg 1. \end{cases} \tag{5.115}$$

Notice the unphysical negative solution has been dropped out.

In some cases, both first- and second-order SSC components may be considered. Assuming no Klein–Nishina correction for both SSC components, one can solve for Y as follows (Kobayashi et al., 2007).

Noting

$$\frac{L_{\rm SSC,2}}{L_{\rm syn}} = \frac{U_{\rm SSC,1}}{U_B} = \frac{U_{\rm SSC,1}}{U_{\rm syn}} \cdot \frac{U_{\rm syn}}{U_B} = Y^2, \tag{5.116}$$

one can write

$$Y \equiv \frac{L_{\rm SSC,1}}{L_{\rm syn}} = \frac{U_{\rm syn}}{U_B} = \frac{\eta_e U_e/(1+Y+Y^2)}{U_B}. \tag{5.117}$$

One therefore needs to solve the equation

$$Y \epsilon_B (1+Y+Y^2) = \eta_e \epsilon_e. \tag{5.118}$$

In the asymptotic regimes, one has

$$Y \simeq \begin{cases} \frac{\eta_e \epsilon_e}{\epsilon_B}, & Y \ll 1, \\ \left(\frac{\eta_e \epsilon_e}{\epsilon_B}\right)^{1/3}, & Y \gg 1. \end{cases} \tag{5.119}$$

5.2.4 SSC Spectrum

In this subsection, we limit ourselves to the case with only the first-order SSC component with no Klein–Nishina correction. Some approximate analytical expressions of the SSC spectral shape are presented. For the cases with a significant Klein–Nishina correction in the first-order SSC component, analytical approximations are available for some spectral regimes discussed below, and we refer the readers to Nakar et al. (2009) for a full treatment of the Klein–Nishina effect. For more general treatments with higher order SSC components and Klein–Nishina corrections, numerical calculations are needed.

From the IC volume emissivity (Eq. (5.98)), one can derive the general form of the observed IC flux (Sari and Esin, 2001):

$$F_\nu^{\rm IC} = \Delta' \sigma_{\rm T} \int_{\gamma_m}^{\infty} d\gamma N(\gamma) \int_0^{x_0} dx F_\nu(x), \tag{5.120}$$

where $F_\nu(x)$ is the specific synchrotron flux, Δ' is the comoving size of the emission region, and the value $x_0 \sim 0.5$ is introduced to ensure energy conservation, i.e. $\int_0^1 xf(x)dx = \int_0^{x_0} xdx$, and x and $f(x)$ are defined in Eqs. (5.96) and (5.95), respectively. One can see that the IC spectrum is a convolution of electron distribution and incident photon spectrum. For a single power-law distribution of electrons, the resulting IC spectrum is also a power law. However, when the electrons have a broken power-law distribution, the SSC spectrum strictly speaking is no longer a broken power law. At high energies, generally there is an additional factor that contains a logarithmic term (Sari and Esin, 2001).

The approximate analytical SSC spectra corresponding to all six synchrotron spectra presented in §5.1.8 were worked out by Gao et al. (2013c). The cases for regimes (I) and (III) were published by Sari and Esin (2001), with two typos corrected by Gao et al. (2013c). We present the results below following Gao et al. (2013c), and the νF_ν spectra of both synchrotron and SSC components (with the normalized flux) are presented in Fig. 5.6. The convention

$$\nu_{ij}^{\rm IC} = 4\gamma_i^2 \nu_j x_0 \tag{5.121}$$

has been adopted, with the subcripts $i, j = a, c, m$ denoting self-absorption, cooling, and minimum injection, respectively, for both Lorentz factor (γ_i) and frequency (ν_i). The electron scattering optical depth τ_{es} (Eq. (5.92)) has been adopted.

Case I: $\nu_a < \nu_m < \nu_c$:

$$F_\nu^{\rm IC} \simeq \tau_{\rm es} F_{\nu,\max} x_0 \tag{5.122}$$
$$\times \begin{cases} \frac{5}{2}\frac{(p-1)}{(p+1)} \left(\frac{\nu_a}{\nu_m}\right)^{\frac{1}{3}} \left(\frac{\nu}{\nu_{ma}^{\rm IC}}\right), & \nu < \nu_{ma}^{\rm IC}; \\ \frac{3}{2}\frac{(p-1)}{(p-1/3)} \left(\frac{\nu}{\nu_{mm}^{\rm IC}}\right)^{\frac{1}{3}}, & \nu_{ma}^{\rm IC} < \nu < \nu_{mm}^{\rm IC}; \\ \frac{(p-1)}{(p+1)} \left(\frac{\nu}{\nu_{mm}^{\rm IC}}\right)^{\frac{1-p}{2}} \left[\frac{4(p+1/3)}{(p+1)(p-1/3)} + \ln\left(\frac{\nu}{\nu_{mm}^{\rm IC}}\right)\right], & \nu_{mm}^{\rm IC} < \nu < \nu_{mc}^{\rm IC}; \\ \frac{(p-1)}{(p+1)} \left(\frac{\nu}{\nu_{mm}^{\rm IC}}\right)^{\frac{1-p}{2}} \left[\frac{2(2p+3)}{(p+2)} - \frac{2}{(p+1)(p+2)} + \ln\left(\frac{\nu_{cc}^{\rm IC}}{\nu}\right)\right], & \nu_{mc}^{\rm IC} < \nu < \nu_{cc}^{\rm IC}; \\ \frac{(p-1)}{(p+1)} \left(\frac{\nu}{\nu_{mm}^{\rm IC}}\right)^{-\frac{p}{2}} \left(\frac{\nu_c}{\nu_m}\right) \left[\frac{2(2p+3)}{(p+2)} - \frac{2}{(p+2)^2} + \frac{(p+1)}{(p+2)} \ln\left(\frac{\nu}{\nu_{cc}^{\rm IC}}\right)\right], & \nu > \nu_{cc}^{\rm IC}. \end{cases}$$

Case II: $\nu_m < \nu_a < \nu_c$:

$$F_\nu^{\rm IC} \simeq \tau_{\rm es} F_{\nu,\max} x_0 \times \begin{cases} \frac{2(p+4)(p-1)}{3(p+1)^2}\left(\frac{\nu_m}{\nu_a}\right)^{\frac{p+1}{2}}\left(\frac{\nu}{\nu_{mm}^{\rm IC}}\right), & \nu < \nu_{ma}^{\rm IC}; \\ \frac{(p-1)}{(p+1)}\left(\frac{\nu}{\nu_{mm}^{\rm IC}}\right)^{\frac{1-p}{2}}\left[\frac{2(2p+5)}{(p+1)(p+4)}+\ln\left(\frac{\nu}{\nu_{ma}^{\rm IC}}\right)\right], & \nu_{ma}^{\rm IC} < \nu < \nu_{mc}^{\rm IC}; \\ \frac{(p-1)}{(p+1)}\left(\frac{\nu}{\nu_{mm}^{\rm IC}}\right)^{\frac{1-p}{2}}\left[2+\frac{2}{p+4}+\ln\left(\frac{\nu_c}{\nu_a}\right)\right], & \nu_{mc}^{\rm IC} < \nu < \nu_{ca}^{\rm IC}; \\ \frac{(p-1)}{(p+1)}\left(\frac{\nu}{\nu_{mm}^{\rm IC}}\right)^{\frac{1-p}{2}}\left[\frac{2(2p+1)}{(p+1)}+\ln\left(\frac{\nu_{cc}^{\rm IC}}{\nu}\right)\right], & \nu_{ca}^{\rm IC} < \nu < \nu_{cc}^{\rm IC}; \\ \frac{(p-1)}{(p+2)}\left(\frac{\nu_c}{\nu_m}\right)\left(\frac{\nu}{\nu_{mm}^{\rm IC}}\right)^{-\frac{p}{2}}\left[\frac{2(2p+5)}{(p+2)}+\ln\left(\frac{\nu}{\nu_{cc}^{\rm IC}}\right)\right], & \nu > \nu_{cc}^{\rm IC}. \end{cases} \tag{5.123}$$

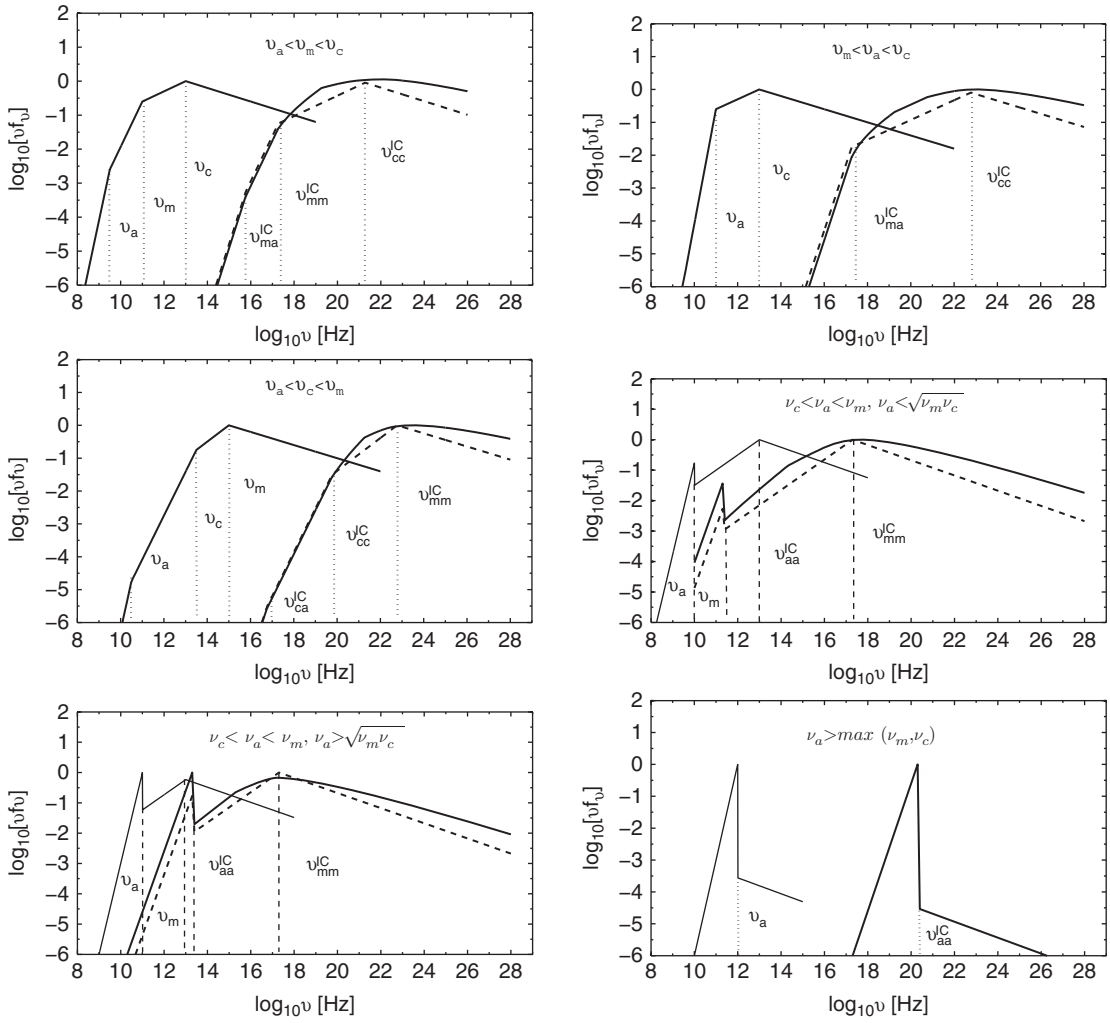

Figure 5.6 Synchrotron and SSC νF_ν spectra of electrons with different orders of ν_a, ν_m, and ν_c. From top left to bottom right: (I) $\nu_a < \nu_m < \nu_c$; (II) $\nu_m < \nu_a < \nu_c$; (III) $\nu_a < \nu_c < \nu_m$; (IV) $\nu_c < \nu_a < \nu_m$, non-thermal dominated; (IV) $\nu_c < \nu_a < \nu_m$, thermal dominated; (V) and (VI) $\nu_a > \max(\nu_m, \nu_c)$. For strong absorption (electron pile-up) cases (IV–VI), a very rough approximation of the pile-up spectrum is adopted to allow a power-law description of the spectra. See text for details. Adapted from Gao et al. (2013c).

Case III: $\nu_a < \nu_c < \nu_m$:

$$F_\nu^{\rm IC} \simeq \tau_{\rm es} F_{\nu,\max} x_0 \times \begin{cases} \frac{5}{6}\left(\frac{\nu_a}{\nu_c}\right)^{\frac{1}{3}}\left(\frac{\nu}{\nu_{ca}^{\rm IC}}\right), & \nu < \nu_{ca}^{\rm IC}; \\ \frac{9}{10}\left(\frac{\nu}{\nu_{cc}^{\rm IC}}\right)^{\frac{1}{3}}, & \nu_{ca}^{\rm IC} < \nu < \nu_{cc}^{\rm IC}; \\ \frac{1}{3}\left(\frac{\nu}{\nu_{cc}^{\rm IC}}\right)^{-\frac{1}{2}}\left[\frac{28}{15} + \ln\left(\frac{\nu}{\nu_{cc}^{\rm IC}}\right)\right], & \nu_{cc}^{\rm IC} < \nu < \nu_{cm}^{\rm IC}; \\ \frac{1}{3}\left(\frac{\nu}{\nu_{cc}^{\rm IC}}\right)^{-\frac{1}{2}}\left[\frac{2(p+5)}{(p+2)(p-1)} - \frac{2(p-1)}{3(p+2)} + \ln\left(\frac{\nu_{mm}^{\rm IC}}{\nu}\right)\right], & \nu_{cm}^{\rm IC} < \nu < \nu_{mm}^{\rm IC}; \\ \frac{1}{(p+2)}\left(\frac{\nu_c}{\nu_m}\right)\left(\frac{\nu}{\nu_{mm}^{\rm IC}}\right)^{-\frac{p}{2}}\left[\frac{2}{3}\frac{(p+5)}{(p-1)} - \frac{2}{3}\frac{(p-1)}{(p+2)} + \ln\left(\frac{\nu}{\nu_{mm}^{\rm IC}}\right)\right], & \nu > \nu_{mm}^{\rm IC}. \end{cases} \tag{5.124}$$

For $\nu_a < \nu_m < \nu_c$ (case I) and $\nu_m < \nu_a < \nu_c$ (case II), the νF_ν peaks of the synchrotron and SSC components are at ν_c and ν_{cc}^{IC}, respectively. One can estimate

$$Y = \frac{L_{\rm IC}}{L_{\rm syn}} \sim 4x_0^2\tau_{\rm es}\gamma_c^2\left(\frac{\gamma_c}{\gamma_m}\right)^{1-p}. \tag{5.125}$$

For $\nu_a < \nu_c < \nu_m$ (case III), the νF_ν peaks of the synchrotron and SSC components are at ν_m and $\nu_{mm}^{\rm IC}$, respectively. One therefore has

$$Y = \frac{L_{\rm IC}}{L_{\rm syn}} \sim 4x_0^2\tau_{\rm es}\gamma_c\gamma_m. \tag{5.126}$$

The above three regimes are the weak absorption cases, for which the synchrotron spectra are well described as broken power laws. In the strong absorption regimes, the synchrotron spectra show a quasi-thermal peak due to electron pile-up. The SSC spectra also correspondingly show two (quasi-thermal vs. broken power-law) components. The following approximate formulae are based on a rough approximation of the synchrotron spectra (§5.1.8). Numerical calculations are needed to reach a more precise result.

Case IV: $\nu_c < \nu_a < \nu_m$:

$$F_\nu^{\rm IC} \simeq \tau_{\rm es} F_{\nu,\max} x_0 \times \begin{cases} \left(\frac{1}{2}\mathcal{R}+1\right)(\mathcal{R}+4)\left(\frac{\nu}{\nu_{aa}^{\rm IC}}\right), & \nu < \nu_{aa}^{\rm IC}; \\ \mathcal{R}\left(\frac{\nu}{\nu_{aa}^{\rm IC}}\right)^{-\frac{1}{2}}\left[\frac{1}{6}\mathcal{R} + \frac{9}{10} + \frac{1}{4}\mathcal{R}\ln\left(\frac{\nu}{\nu_{aa}^{\rm IC}}\right)\right], & \nu_{aa}^{\rm IC} < \nu < \nu_{am}^{\rm IC}; \\ \mathcal{R}^2\left(\frac{\nu}{\nu_{aa}^{\rm IC}}\right)^{-\frac{1}{2}}\left[\frac{3}{p-1} - \frac{1}{2} + \frac{3}{4}\ln\left(\frac{\nu_{mm}^{\rm IC}}{\nu}\right)\right], & \nu_{am}^{\rm IC} < \nu < \nu_{mm}^{\rm IC}; \\ \frac{9}{2(p+2)}\mathcal{R}^2\left(\frac{\nu_a}{\nu_m}\right)\left(\frac{\nu}{\nu_{mm}^{\rm IC}}\right)^{-\frac{p}{2}} \\ \quad\times\left[\frac{4}{p+3}\left(\frac{\gamma_a}{\gamma_m}\right)^{p-1}\frac{\gamma_a}{\gamma_c} + \frac{3(p+1)}{(p-1)(p+2)} + \frac{1}{2}\ln\frac{\nu}{\nu_{mm}^{\rm IC}}\right], & \nu > \nu_{mm}^{\rm IC}. \end{cases} \tag{5.127}$$

Here $\mathcal{R}$ is defined in Eq. (5.65).

For this case, there are two peaks in both the synchrotron and SSC νF_ν spectra (Fig. 5.6). The spectrum is thermal (non-thermal) dominated if $\nu_a > \sqrt{\nu_m\nu_c}$ ($\nu_a < \sqrt{\nu_m\nu_c}$). In the non-thermal-dominated regime, the synchrotron and SSC emission components peak at ν_m and $\nu_m^{\rm IC}$, respectively, with

$$Y = \frac{L_{\rm IC}}{L_{\rm syn}} 4x_0^2 \tau_{es} \gamma_c \gamma_m. \tag{5.128}$$

In the thermal-dominated regime, the synchrotron and SSC emission components peak at ν_a and $\nu_a^{\rm IC}$, respectively, with

$$Y = \frac{L_{\rm IC}}{L_{\rm syn}} 4x_0^2 \tau_{\rm es} \gamma_a^2. \tag{5.129}$$

More generally, in this regime, one can write

$$Y = \frac{L_{\rm IC}}{L_{\rm syn}} 4x_0^2 \tau_{es} \max(\gamma_a^2, \gamma_c \gamma_m). \tag{5.130}$$

Cases V and VI: $\nu_a > \max(\nu_m, \nu_c)$:

$$F_\nu^{\rm IC} \simeq \tau_{\rm es} F_{\nu,\max} x_0 \tag{5.131}$$
$$\times \begin{cases} \left(\frac{3\mathcal{R}}{2(p+2)} + 1\right)\left(\frac{3\mathcal{R}}{p+2} + 4\right)\left(\frac{\nu}{\nu_{aa}^{\rm IC}}\right), & \nu < \nu_{aa}^{\rm IC}; \\ \frac{1}{p+2}\left[\frac{6\mathcal{R}}{p+3} + \mathcal{R}\left(\frac{9\mathcal{R}}{2(p+2)} + 1\right) + \frac{9\mathcal{R}^2}{4}\ln\left(\frac{\nu}{\nu_{aa}^{\rm IC}}\right)\right]\left(\frac{\nu}{\nu_{aa}^{\rm IC}}\right)^{-\frac{p}{2}}, & \nu > \nu_{aa}^{\rm IC}; \end{cases}$$

where $\mathcal{R}$ is defined in Eqs. (5.66) and (5.67) for regimes V and IV, respectively.

In this regime, one has

$$Y = \frac{L_{\rm IC}}{L_{\rm syn}} \sim 4x_0^2 \tau_{\rm es} \gamma_a^2. \tag{5.132}$$

5.2.5 Multiple Inverse Compton Scattering

In some GRB problems (e.g. emission from a *dissipative photosphere*), thermal photons from deep in the fireball would undergo multiple scatterings by the electrons at a range of optical depths near the photosphere. In these problems, multiple IC scattering is relevant.

Compton y Parameter

To treat the multiple Compton scattering problem a parameter known as the *Compton y parameter* is highly relevant. This factor is defined as

$$y = \frac{\langle \Delta\epsilon \rangle}{\epsilon} \cdot \langle N_{\rm es} \rangle, \tag{5.133}$$

where $\langle \epsilon \rangle / \epsilon$ is the average fractional energy change per scattering, and $\langle N_{\rm es} \rangle$ is the mean number of scatterings (Rybicki and Lightman, 1979). It describes how efficient seed photons gain energy from electrons. For single scattering, as discussed earlier, one has $\Delta\epsilon = \epsilon_1 - \epsilon \simeq (\gamma^2 - 1)\epsilon \sim \gamma^2 \epsilon$, and $\langle N_{\rm es} \rangle \sim \tau_{\rm es} \ll 1$, so that

$$y \sim \gamma^2 \tau_{\rm es}. \tag{5.134}$$

Notice that the parameter Y introduced in §5.2.3 is close to y, but in some regimes is not exactly the same (see §5.2.4 for detailed derivations of Y for different spectral regimes).

We consider the problem of a seed photon field propagating through an electron gas. With the GRB fireball picture in mind, the seed photons are assumed to have a blackbody

distribution defined by a temperature $T_{\rm ph}$. If the electrons have a thermal distribution with temperature $T_e = T_{\rm ph}$, then the photons and electrons are in thermal equilibrium, and the emergent photon spectrum is not modified.

A more interesting and relevant problem is that the electron gas has a higher temperature $T_e > T_{\rm ph}$ or does not have a thermal distribution at all. Through multiple scatterings, seed photons progressively gain energy from the electrons, so that the emergent photon spectrum deviates from the original blackbody form. This process is also called *Comptonization*. It is called *up-Comptonization* if $T_e > T_{\rm ph}$, and vice versa *down-Comptonization*. For GRB dissipative photosphere problems, one deals with the up-Comptonization problem.

Let us assume that electrons are in thermal equilibrium with $T_e > T_{\rm ph}$. The average fractional energy change per scattering reads (Rybicki and Lightman, 1979)

$$\frac{\langle \Delta\epsilon \rangle}{\epsilon} \simeq \begin{cases} \frac{(4kT_e - \epsilon)}{m_e c^2}, & kT_e \ll m_e c^2 \text{ (non-relativistic)}, \\ \frac{4}{3}\gamma_e^2 \epsilon \simeq 16 \left(\frac{kT_e}{m_e c^2}\right)^2, & kT_e \gg m_e c^2 \text{ (relativistic)}. \end{cases} \tag{5.135}$$

The average number of scatterings depends on the Thomson scattering optical depth $\tau_{\rm es}$ (Eq. (5.92)). For $\tau_{\rm es} \gg 1$, the average number of scatterings is $\langle N_{\rm es} \rangle \sim \tau_{\rm es}^2$ due to the random walk of the photons; for $\tau_{\rm es} \ll 1$, the average number of scatterings $\langle N_{\rm es} \rangle$ is simply $\tau_{\rm es}$. Putting everything together, one has

$$y \sim \max\left(\frac{(4kT_e - \epsilon)}{m_e c^2}, 16 \left(\frac{kT_e}{m_e c^2}\right)^2 \right) \times \max(\tau_{\rm es}, \tau_{\rm es}^2). \tag{5.136}$$

For electrons with a distribution not fully thermal, the above equation is still approximately valid given that kT_e is replaced by the mean energy of the electrons.

Comptonized Spectrum

Deriving a Comptonized spectrum requires solving the Boltzmann equation of photon density in energy space, $n(\omega)$, by considering processes scattering into and out of angular frequency ω. The treatment is lengthy and complicated (see Rybicki and Lightman 1979 and references therein). Here we only summarize some well-known results (see also Ghisellini, 2013; Kumar and Zhang, 2015).

We assume that the seed photons have a *blackbody* spectrum:

$$I_\nu = B_\nu(T_{\rm ph}) \equiv \frac{2}{c^2} \frac{h\nu^3}{e^{h\nu/kT_{\rm ph}} - 1}. \tag{5.137}$$

For $h\nu \ll kT_{\rm ph}$, one has the *Rayleigh–Jeans law*:

$$I_\nu \simeq \frac{2\nu^2}{c^2} kT_{\rm ph} \propto \nu^2; \tag{5.138}$$

and for $h\nu \gg kT_{\rm ph}$, one has the *Wien law*:

$$I_\nu \simeq \frac{2h\nu^3}{c^2} e^{-h\nu/kT_{\rm ph}}, \tag{5.139}$$

characterized by an exponential cutoff. The shape of the emergent Comptonization spectrum depends on the values of $\tau_{\rm es}$ and y. One may discuss the following regimes:

- $y \ll 1$, $\tau_{\rm es} < 1$: In this case, the seed photons gain little energy. The spectrum below the peak remains Rayleigh–Jeans. Above the peak, due to multiple scattering, a power law is developed. The reason is that, for each scattering, a photon gains an energy $\Delta\epsilon$. The more scatterings the photon has, the more energy it gains, but in the meantime the number of scatterings drops (since $\tau_{\rm es} < 1$). Defining

$$A_f = \frac{\langle \Delta\epsilon \rangle + \epsilon_0}{\epsilon_0} \simeq \max\left(\frac{4kT_e}{m_e c^2}, 16\left(\frac{kT_e}{m_e c^2}\right)^2\right) \simeq \frac{y}{\tau_{\rm es}}, \tag{5.140}$$

  the spectral index above the Comptonized thermal peak (in the convention of $F_\nu \propto \nu^{-\beta}$) is

$$\beta = \frac{-\log \tau_{\rm es}}{\log A_f}, \tag{5.141}$$

  since, on a logarithmic scale, the fraction of photons whose energy increases by $\log A_f$ is $-\log \tau_{\rm es}$. One has $\beta \sim 1$ when $y \sim 1$. It becomes harder ($\beta < 1$) when $y > 1$, and vice versa. Notice that, when $\tau_{\rm es} \ll 1$ and $A_f \gg 1$, the spectrum is characterized by "bumps" of individual scattering orders.
- $y \gg 1$, $\tau_{\rm es} \gg 1$: This is the regime of *saturation*. The interactions between photons and electrons are so intense that they reach equilibrium, i.e. the emergent photon spectrum has a temperature of T_e. However, since scatterings conserve photon number, moving the original blackbody spectrum to a higher temperature means that the low-frequency regime deviates from the Rayleigh–Jeans ($F_\nu \propto \nu^2$) regime. The spectrum will take the Wien shape with $F_\nu \propto \nu^3$ (Eq. 5.139).
- $y \sim 1$, $\tau_{\rm es} \gtrsim 1$: This is the intermediate, unsaturated Comptonization regime. The solution is most complicated. One needs to solve the so-called "Kompaneets" equation in the photon energy space $x = h\nu/kT_e$,

$$\frac{\partial n}{\partial t_c} = \left(\frac{kT_e}{m_e c^2}\right)\frac{1}{x^2}\frac{\partial}{\partial x}\left[x^4(n' + n + n^2)\right], \tag{5.142}$$

  where $t_c \equiv (n_e \sigma_{\rm T} c)t = t/t_{\rm es}$ is the time in units of the mean time between scatterings, $t_{\rm es}$.

5.2.6 Double Compton Scattering

The inverse Compton scattering processes discussed so far conserve the total number of photons. In a high n_γ/n_e and optically thick environment (i.e. photons are much more abundant than electrons, and $\tau_{\rm es} \gg 1$), the so-called double Compton (DC) emission (Thorne, 1981; Lightman, 1981),

$$p + \gamma \rightleftharpoons p + \gamma + \gamma, \tag{5.143}$$

is possible. The right arrow denotes a photon generation mechanism, which is relevant for GRB fireballs deep below the photosphere. Scattering of mono-energetic photons with

energy $h\nu_0$ and density n_γ by cold electrons with number density n_e produces secondary photons $h\nu$ with the differential photon generation rate given by

$$\frac{d\dot{n}_{\rm DC}}{d\ln\nu} = \frac{4\alpha_f}{3\pi} n_e n_\gamma \sigma_{\rm T} c \left(\frac{h\nu_0}{m_e c^2}\right)^2, \tag{5.144}$$

where $\alpha_f = e^2/\hbar c \simeq 1/137$ is the fine structure constant.

For a Bose–Einstein photon field with temperature T, the differential photon generation rate may be written (Beloborodov, 2013)

$$\frac{d\dot{n}_{\rm DC}}{d\ln x} = \frac{4\alpha_f}{3\pi} n_e n_\gamma \sigma_{\rm T} c \bar{x}_0^2 \Theta^2, \tag{5.145}$$

where $x_0 = h\nu_0/kT$, $x = h\nu/kT$, $\Theta = kT/m_e c^2$, and $\bar{x}_0^2 \simeq 10.35$ for a Planck spectrum and $\bar{x}_0^2 = 12$ for a Wien spectrum.

Integration over $d\ln x$ gives (Beloborodov, 2013)

$$\dot{n}_{\rm DC} = \chi n_e n_\gamma \sigma_{\rm T} c \Theta^2, \tag{5.146}$$

where $\chi = (4\alpha_f/3\pi)\bar{x}_0^2 \ln x_{\rm min}^{-1}$.

In a $n_\gamma/n_e \gg 1$, $\tau_{\rm es} \gg 1$ environment (deep below a GRB fireball photosphere), this photon generation process continuously generates new photons until a Planck distribution is reached, after which the inverse process (double Compton absorption) kicks in to maintain the Planck distribution of the photons.

5.2.7 Inverse Compton Polarization

Thomson scattering is intrinsically polarized, and so is inverse Compton scattering. For a single scattering event, the polarization degree due to IC is (Rybicki and Lightman 1979)

$$\Pi = \frac{1-\cos^2\theta}{1+\cos^2\theta}, \tag{5.147}$$

where θ is the angle between the incoming photon and the outgoing photon. The maximum polarization $\Pi \sim 100\%$ is achievable when $\theta = \pi/2$.

5.3 Bremsstrahlung

Bremsstrahlung is also called *free–free radiation*. It is the emission from unbound electrons in the Coulomb electric field of ions/nuclei. It is an important electron emission mechanism in dense plasma. The process may be written as

$$e + p \to e + p + \gamma. \tag{5.148}$$

A *relativistic bremsstrahlung* process may be regarded as an electron scattering off a virtual quanta of the ion's electrostatic field as seen in the electron's comoving frame. With an additional vertex in the Feynman scattering diagram (Jauch and Rohrlich, 1976), the

cross section of relativistic bremsstrahlung is smaller than the Thomson cross section by a factor of the fine structure constant $\alpha_f = e^2/\hbar c \simeq 1/137$, i.e.

$$\sigma_{\rm brem} \sim \alpha_f \sigma_{\rm T}. \tag{5.149}$$

For a fully ionized plasma, the relativistic electron bremsstrahlung energy loss rate is given by (Blumenthal and Gould, 1970)

$$\dot{\gamma}_{\rm brem} = -\frac{3}{2\pi}\alpha_f \sigma_{\rm T} c \gamma \left(\ln 2\gamma - \frac{1}{3}\right)\left(\sum_Z n_Z Z(Z+1)\right), \tag{5.150}$$

where Z stands for the atomic number of ion species in the plasma. For our purpose, we consider a fully ionized hydrogen plasma, and approximate the energy loss rate as

$$\dot{\gamma}_{\rm brem} \sim -\alpha_f \sigma_{\rm T} c \gamma n_p, \tag{5.151}$$

where n_p is the number density of the protons. For comparison, the energy loss rates of synchrotron and IC are, respectively,

$$\dot{\gamma}_{\rm syn} \sim -\frac{4}{3}\frac{\sigma_{\rm T} c \gamma^2 U_B}{m_e c^2}, \tag{5.152}$$

$$\dot{\gamma}_{\rm IC} \sim -\frac{4}{3}\frac{\sigma_{\rm T} c \gamma^2 U_{\rm ph}}{m_e c^2}. \tag{5.153}$$

One may also compare the radiation power of the three mechanisms:

$$P_{\rm brem} \sim \alpha_f \sigma_{\rm T} c \gamma n_p m_e c^2, \tag{5.154}$$

$$P_{\rm syn} \sim \frac{4}{3}\sigma_{\rm T} c \gamma^2 U_B, \tag{5.155}$$

$$P_{\rm IC} \sim \frac{4}{3}\sigma_{\rm T} c \gamma^2 U_{\rm ph}. \tag{5.156}$$

It is informative to compare the relative importance between the synchrotron power and the bremsstrahlung power:

$$\frac{P_{\rm syn}}{P_{\rm brem}} \sim \frac{\gamma U_B}{\alpha_f n_p m_e c^2} = \frac{m_p}{m_e}\frac{\gamma}{\alpha_f}\sigma \simeq 2.5 \times 10^5 \gamma \sigma, \tag{5.157}$$

where

$$\sigma \equiv \frac{U_B}{\rho c^2} \tag{5.158}$$

is the magnetization parameter of the flow, and $\rho = n_p m_p$ is the matter density of the hydrogen plasma.

In GRB problems, the typical electron Lorentz factor is $\gamma \gg 1$. The magnetization parameter σ is not small. For prompt emission, σ is suggested to be about 2 orders of magnitude centered around unity (see Chapter 9 for details). For afterglow emission, $\sigma \sim \epsilon_B \ll 1$, but is usually not small enough to compensate the $(2.5 \times 10^5 \gamma)$ factor in Eq. (5.157). As a result, the ratio $P_{\rm syn}/P_{\rm brem}$ should be $\gg 1$ in most GRB problems.

Bremsstrahlung is discussed in GRB photosphere problems as one photon generation (and absorption) mechanism at very high optical depth (Beloborodov, 2013; Vurm et al.,

2013). Defining $x = h\nu/kT$ and $\Theta = kT/m_e c^2$, the differential bremsstrahlung photon generation rate is given by (Illarionov and Siuniaev, 1975; Thorne, 1981)

$$\frac{d\dot{n}_{\gamma,\rm brem}}{d\ln x} = \left(\frac{2}{\pi}\right)^{3/2} \alpha_f n_p^2 \sigma_{\rm T} c \Theta^{-1/2} \ln\frac{2.2}{x}. \tag{5.159}$$

Integration over $\ln x$ from $\ln x_{\rm min}$ to $\ln x \sim 0$ gives (Beloborodov, 2013)

$$\dot{n}_{\gamma,\rm brem} = \xi n_p^2 \sigma_{\rm T} c \Theta^{-1/2}, \tag{5.160}$$

where $\xi \simeq (2/\pi)^{3/2}\alpha_f (\ln x_{\rm min}^{-1})^2 \sim 0.06$.

5.4 Pair Production and Annihilation

Within the framework of QED, Compton scattering, photon–photon pair production, and pair annihilation share the same Feynman diagram, which describes the electromagnetic interaction between charged leptons through exchanging photons.

5.4.1 Two-Photon Pair Production

The electron rest mass energy is $m_e c^2 = 511$ keV. A photon with energy $\geq 2m_e c^2 \sim 1.022$ MeV can be converted to electron–positron pairs. According to QED, a photon with such a high energy turns into "virtual" $e^{\pm}$ pairs all the time, but the pairs quickly convert back to a photon that is identical to the original one. In order to "materialize" a photon, another agent has to be involved to conserve both energy and momentum. This second party can be either another photon, an electric field, or a magnetic field.

We first consider the so-called two-photon pair production ($\gamma\gamma \to e^+e^-$) process.

Kinematics

For a relativistic particle, energy and momentum can be written as

$$E = mc^2 = \gamma m_0^2 c^2, \tag{5.161}$$

$$\mathrm{p} = mv = \gamma m_0 \beta c, \tag{5.162}$$

so that

$$E^2 - \mathrm{p}^2 c^2 = \gamma^2 m_0^2 c^4 - \gamma^2 m_0^2 \beta^2 c^4 = m_0^2 c^4 \gamma^2 (1-\beta^2) = m_0^2 c^4 = \text{const.} \tag{5.163}$$

This quantity, a *relativistic invariant*, does not depend on the rest frame, and carries the physical meaning of the square of the rest mass energy of the particle. For photons, one has $E = h\nu$, and $\mathrm{p} = h\nu/c$, so that

$$E^2 - \mathrm{p}^2 c^2 = 0, \tag{5.164}$$

i.e. the rest mass is zero.

For a general reaction process, the relativistic invariant before and after the reaction should be conserved. Taking the two-photon pair production process, i.e. $\gamma_1\gamma_2 \to e^+e^-$, as an example, one has

$$(E_{\gamma,1} + E_{\gamma,2})^2 - (\mathrm{p}_{\gamma,1} + \mathrm{p}_{\gamma,2})^2 c^2 = (E_{e^+} + E_{e^-})^2 - (\mathrm{p}_{e^+} + \mathrm{p}_{e^-})^2 c^2. \tag{5.165}$$

At the threshold, the produced pair of particles equally share the total energy and momentum of the incoming two photons, so that one has $E_{e^+} = E_{e^-} = E$ and $\mathrm{p}_{e^+} = \mathrm{p}_{e^-} = \mathrm{p}$. The right hand side of Eq. (5.165) then becomes $(2E)^2 - (2\mathrm{p})^2 c^2 = 4m_e^2 c^4$.

Now consider the two photons with $E_{\gamma,1} = h\nu_1$, $E_{\gamma,2} = h\nu_2$, and an incident angle θ; the left hand side of Eq. (5.165) then becomes $2E_{\gamma,1}E_{\gamma,2} - 2\mathrm{p}_{\gamma,1}\cdot\mathrm{p}_{\gamma,2}c^2 = 2h\nu_1\cdot h\nu_2(1-\cos\theta)$. Therefore the *kinematic condition* can be written as (Exercise 5.5)

$$h\nu_1 \cdot h\nu_2(1 - \cos\theta) \geq 2(m_e c^2)^2, \tag{5.166}$$

with the equal sign denoting the *threshold condition*. Taking $\cos\theta = -1$, one gets the threshold condition for two-photon pair production:

$$h\nu_1 \cdot h\nu_2 \geq (m_e c^2)^2. \tag{5.167}$$

Cross Section

In the center-of-momentum frame (S_0), the cross section can be written conveniently as (Jauch and Rohrlich, 1976)

$$\sigma_{\gamma\gamma} = \frac{1}{2}\pi r_0^2(1-\beta_\pm^2)\left[(3-\beta_\pm^4)\ln\frac{1+\beta_\pm}{1-\beta_\pm} - 2\beta_\pm(2-\beta_\pm^2)\right], \tag{5.168}$$

where $\beta_\pm$ is the dimensionless velocity of e^+, e^- in the S_0 frame, and r_0 (Eq. (5.86)) is the classical electron radius. The parameter $\beta_\pm$ can be written in terms of the incoming photon energy $h\nu_0$, which is identical for the two photons in S_0:

$$\beta_\pm = \frac{v}{c} = \frac{c\mathrm{p}}{E_0} = \sqrt{1 - \left(\frac{m_e c^2}{h\nu_0}\right)^2}, \tag{5.169}$$

where $c^2\mathrm{p}^2 = E_0^2 - m_0^2 c^4 = (h\nu_0)^2 - m_e^2 c^4$ has been used.

The Lorentz factor of the outgoing pairs is

$$\gamma_\pm \equiv \frac{h\nu_0}{m_e c^2}, \tag{5.170}$$

so the cross section can be re-written as

$$\sigma_{\gamma\gamma} = \pi r_0^2 \gamma_\pm^{-2}\left[(2 + 2\gamma_\pm^{-2} - \gamma_\pm^{-4})\ln\left|\gamma_\pm - \sqrt{\gamma_\pm^2 - 1}\right| - \sqrt{1-\gamma_\pm^{-2}}(1+\gamma_\pm^{-2})\right]. \tag{5.171}$$

When $\beta_\pm \ll 1$, $h\nu_0 \lesssim m_e c^2$, $\gamma_\pm \sim 1$, one has

$$\sigma^{\gamma\gamma\to e^+e^-} = \pi r_0^2 \beta_\pm. \tag{5.172}$$

When $\beta_\pm \lesssim 1$, $h\nu_0 \gg m_e c^2$, $\gamma_\pm \gg 1$, one has

$$\sigma^{\gamma\gamma\to e^+e^-} = \pi r_0^2 \gamma_\pm^{-2}(\ln 2\gamma_\pm^2 - 1). \tag{5.173}$$

One can see that the cross section decreases in both the non-relativistic regime ($\beta_\pm \ll 1$) and the relativistic regime ($\gamma_\pm \gg 1$). It is largest in the trans-relativistic regime, i.e. $\beta_\pm \sim 1$ and $\gamma_\pm \sim 1$.

This two-photon pair production process plays an important role in GRB problems.

5.4.2 One-Photon Pair Production

One high-energy photon can be converted to pairs in either an electric field or a magnetic field.

Pair Production in Coulomb Field: The Bethe–Heitler Process

An energetic photon can materialize in the Coulomb field of an ion. The cross section for a photon to generate a pair in the Coulomb field of a fully ionized ion with atomic number Z is (Bethe and Heitler, 1934)

$$\sigma_{\rm BH} = \begin{cases} 4\alpha_f Z^4 r_0^2 \left[\frac{7}{9}\ln\left(\frac{2h\nu}{m_e c^2}\right) - \frac{109}{54}\right], & \frac{2E_{e^+}E_{e^-}}{h\nu} \ll \frac{m_e c^2}{\alpha_f Z^{1/3}}, \\ 4\alpha_f Z^2 r_0^2 \left[\frac{7}{9}\ln\left(\frac{183}{Z^{1/3}}\right) - \frac{1}{54}\right], & \frac{2E_{e^+}E_{e^-}}{h\nu} \gg \frac{m_e c^2}{\alpha_f Z^{1/3}}. \end{cases} \tag{5.174}$$

Similar to relativistic bremsstrahlung, this cross section is also of order of $\alpha_f \sigma_{\rm T}$.

Pair Production in Magnetic Field ($\gamma B \to e^+e^-B$)

Unlike particles (photons, ions, etc.), one cannot define a "number density" for a magnetic field. Therefore, instead of deriving a cross section, it is more convenient to derive an *absorption coefficient* κ for one-photon pair production in a B field (Erber, 1966):

$$\begin{aligned} \kappa &= \frac{1}{4}\left(\frac{3}{2}\right)^{1/2} \alpha_f \frac{m_0 c}{\hbar}\frac{B_\perp}{B_q}\exp\left[-\frac{8mc^2}{3h\nu}\frac{B_q}{B}\right] \\ &\simeq 10^6\ {\rm cm}^{-1} B_{12}\sin\theta \exp\left[-\frac{60}{\left(\frac{h\nu}{\rm MeV}\right)B_{12}\sin\theta}\right], \end{aligned} \tag{5.175}$$

where $B_q \equiv (m_e^2 c^3)(e\hbar) = 4.414 \times 10^{13}$ G is the critical magnetic field strength at which the electron gyration energy equals its rest mass energy (Eq. (5.52)). The mean free path of a photon before converting to a pair is $l = 1/\kappa$.

Both one-photon pair production processes may be important near the GRB central engine, but the produced pairs would have already annihilated inside the fireball before reaching the photosphere radius (see details in §9.5). In the GRB emission regions, these processes are usually not important.

5.4.3 Pair Annihilation

An electron and a positron can annihilate and emit two photons: $e^+e^- \to \gamma\gamma$.

Consider the rest frame of one particle (say, e^-), and the other particle (say, e^+) moves towards the former with a Lorentz factor γ_r. The cross section for $e^+e^- \to \gamma\gamma$ annihilation is (Jauch and Rohrlich, 1976)

$$\sigma_{e^+e^-} = \frac{\pi r_0^2}{\gamma_r + 1}\left[\frac{\gamma_r^2 + 4\gamma_r + 1}{\gamma_r^2 - 1}\ln\left(\gamma_r + \sqrt{\gamma_r^2 - 1}\right) - \frac{\gamma_r + 3}{\sqrt{\gamma_r^2 - 1}}\right]. \tag{5.176}$$

When $\beta_r \ll 1$ ($\gamma_r \gtrsim 1$), one has

$$\sigma_{e^+e^-} \simeq \pi r_0^2 \beta_r^{-1}. \tag{5.177}$$

When $\gamma_r \gg 1$ ($\beta_r \lesssim 1$), one has

$$\sigma_{e^+e^-} \simeq \frac{\pi r_0^2}{\gamma_r}(\ln 2\gamma_r - 1) \propto \gamma_r^{-1}. \tag{5.178}$$

So annihilation becomes progressively more efficient when the two leptons have progressively smaller relative speed. The annihilation line is therefore always close to the rest mass of the electron:

$$h\nu \simeq m_e c^2 \simeq 511 \text{ keV}. \tag{5.179}$$

Exercises

5.1 Derive the power-law spectrum Eq. (5.13).

5.2 Derive the self-absorption coefficients Eqs. (5.39) and (5.40).

5.3 Derive all six cases of broken power-law spectra for synchrotron radiation in §5.1.8.

5.4 Derive the expressions of Y in the $Y \gg 1$ and $Y \ll 1$ regimes for both the cases with first-order SSC component only (Eq. (5.115)) and with both first- and second-order SSC components (Eq. (5.119)).

5.5 Derive the kinematic condition of the two-photon pair production process (Eq. (5.166)).